Available online at www.jourcc.com

Journal homepage: www.JOURCC.com

Journal of Composites and Compounds

Photodegradation of Ciprofloxacin, Acetaminophen, and Carbamazepine using g-C_3N_4-based materials for water treatment

Sogand Bahadori [a], *Mohammadjavad Sharifianjazi* [b], *Sara Eskandarinezhad* [c, *]

[a] *Department of Chemistry, Kerman Branch, Islamic Azad University, Kerman, Iran*
[b] *Department of Material Engineering, Isfahan University of Technology, Isfahan, Iran*
[c] *Department of Mining and Metallurgy, Yazd University, Yazd, Iran*

A B S T R A C T

Recently, the use of photocatalytic materials has been suggested as a possible method for cleaning up the environment. A new photocatalyst for enhanced oxidation processes based on radicals is graphitic carbon nitride (g-C_3N_4), it is metal-free. g-C_3N_4 is a trendy two-dimensional (2D) photocatalyst with a number of advantages, such as responsiveness to strong stability, low cost, and visible light. In the present review, the synthesis and characterization of g-C_3N_4-based photocatalysts are discussed, along with some of their delegate applications in the treatment of wastewater and water (such as acetaminophen, ciprofloxacin, and carbamazepine removal). Meanwhile, the various methods of modification, including doping, defect introduction, heterojunctions, nanocomposites, and so on, are briefly discussed. The associated mechanisms and pertinent discoveries are also examined. Finally, the difficulties, the need for additional study, and the use of g-C_3N_4-based hybrid membranes are underlined.

Peer review under responsibility of UGPH.

A R T I C L E I N F O R M A T I O N

Article history:
Received 11 April 2023
Received in revised form 03 June 2023
Accepted 27 June 2023

Keywords:
Photocatalyst degradation
Photocatalyst
g-C_3N_4
Ciprofloxacin
Acetaminophen
Carbamazepine

Table of contents

1. Introduction 125
2. G-C_3N_4 Structure attributes and photocatalytic potential for water treatment 126
2.1. Enhancing g-C_3N_4 photocatalysis 127
2.1.1. G-C_3N_4 Synthesis insights 127
2.1.2. Designing advanced of g-C_3N_4 preparation technology 128
2.1.3. Advancements in Synthesis Techniques for g-C_3N_4 Nanocomposites 128
3. g-C_3N_4's photocatalytic mechanism 129
3.1. Improvement of photocatalytic performance of g-C_3N_4 129
3.1.1. Metal or non-metal doping 129
3.1.2. Deposition of metals 130
3.1.3. Heterojunction formulation 130
3.1.4. Adjustment of the structure and regulations of defects 131
4. g-C_3N_4 for pharmaceutical removal from water 131
4.1. Photodegradation of Ciprofloxacin 132
4.2 Photodegradation of Acetaminophen (ACT) 133
4.3 Photodegradation of Carbamazepine 134
5. Conclusions and future perspectives 135

1. Introduction

The technology of photocatalysis possesses immense potential in resolving environmental and energy-related concerns, owing to its ability to transform abundant solar power into chemical energy that can be stored [1, 2]. In the influence of light irradiation, a number of redox reactions may transpire on the photocatalysts's surface. Such reactions involve bacteria disinfection [3], contaminant degradation, N_2 fixation [4], CO_2 reduction to organic fuels [5], division of water to H_2 and O_2, etc. Semiconductors, such as g-C_3N_4 [6], CdS, and TiO_2 [7, 8] are the most prevalent photocatalysts [9]. Nevertheless, the efficacy of pure

* *Corresponding author: Sara Eskandarinezhad; E-mail: s.eskandari.nezhad@gmail.com*

https://doi.org/10.61186/jcc.5.2.6

photocatalysts in photocatalytic performance is generally insufficient to meet practical application demands. Consequently, photocatalytic research has centered on investigating preparation methodologies, modification approaches, and the photocatalytic mechanisms of photocatalysts to achieve outstanding photocatalytic activity on easily synthesized and incredibly long-lasting photocatalysts.

Graphitic carbon nitride (g-C_3N_4) has emerged as a high-potential catalyst in Advanced Oxidation Processes (AOPs) owing to its notable characteristics and versatile applications. Composed of nitrogen and carbon atoms arranged in a graphene-like structure, g-C_3N_4 exhibits a metal-free semiconductor nature with a narrow bandgap (~2.7 eV). This unique property enables superior light absorption, making it an efficient photocatalyst under visible light [10]. Its applications are wide-ranging: g-C_3N_4 displays significant potential in photocatalysis, effectively driving redox reactions to address environmental concerns such as pollutant degradation, water treatment, and CO_2 reduction. Furthermore, its ability to generate reactive oxygen species under light irradiation renders it effective in degrading various contaminants, including organic pollutants and pharmaceuticals, while also disinfecting water by eliminating bacteria and microorganisms [11]. Moreover, g-C_3N_4's photocatalytic properties extend to energy conversion applications, offering promise in the production of hydrogen fuel through the conversion and water splitting of CO_2 into valuable organic compounds. Additionally, its role as a catalyst support or co-catalyst in various chemical processes further enhances its applicability [12]. In this context g-C_3N_4 plays a crucial role in the degradation of specific pharmaceuticals including Ciprofloxacin [13], Acetaminophen [14], and Carbamazepine [15] contaminants for water treatment. The utilization of photocatalytic oxidation to eliminate pharmaceutical drugs from wastewater is seen as an appealing and environmentally sustainable method [16].

g-C_3N_4 is typically synthesized by thermal condensation using nitrogen-rich precursors such as urea, thiourea, melamine, dicyanamide, and cyanimide. The synthesis involves nucleophilic addition, polycondensation, and polymerization reactions. The tectonic unit type formed mainly depends on the reaction processes [17]. Construction of g-C_3N_4 nanostructures to overcome the limitations of pure or bulk g-C_3N_4, various nanostructures of g-C_3N_4 have been fabricated and designed. Hard and soft-template methods are used to order porosity onto bulk g-C_3N_4 and create novel morphologies [18]. G-C_3N_4 -based nanocomposites synthesis in recent years, g-C_3N_4 -based nanocomposites have emerged as potential photocatalysts for organic wastewater treatment. Different methods, such as hydrothermal reactions and sol-gel method, have been studied to construct multifunctional g-C_3N_4 -based hybrids. Sol-gel method involves depositing metal nanoparticles on the g-C_3N_4 surface to form heterostructures, while hydrothermal reactions are used to fabricate g-C_3N_4 -based nanocomposites through hydrolysis and polycond [19]. A comprehensive process of the photocatalytic method comprises three consecutive stages: (1) absorption of light and stimulation in order to generate holes and electrons, (2) the movement of photogenerated holes and electrons from within to the photocatalysts' outer layer; and (3) conversion of adsorbed reactants into products via a redox reaction on the surface of the photocatalyst. Involved in these steps are the fundamental causes for the poor function of pristine photocatalysts. First, photocatalysts absorb only a small portion of the solar spectrum, particularly semiconductors with a wide band gap. Second, a significant number of photogenerated electrons and holes recombine upon transfer to the photocatalyst surface.

Thirdly, there are a limited number of reactant adsorption sites and active reactive oxygen species (ROS) sites on the photocatalyst's surface [20]. Improvement of the photocatalytic performance of g-C_3N_4 included Metal or non-metal doping, Heterojunction formulation , and adjustment of the structure and regulations of defects [21]. The global usage of pharmaceuticals has been steadily rising, leading to the emergence of significant concern regarding the presence of pharmaceuticals and their byproducts in water, posing a potential threat to both animals and humans [22]. Removing these pollutants has become a serious reseach topic. Removing drugs such as Ciprofloxacin, Acetaminophen, and Carbamazepine from water has significant environmental and human benefits, Preserving the health of the environment, the mentioned drugs can threaten the environment as water pollutants. Removing these drugs from water reduces negative effects on aquatic organisms, such as fish and other organisms [23]. Preserving public health, Drinking water containing forgotten drugs may bring risks to humans. These substances may enter the human body through drinking water and cause various side effects. Removing these drugs from water helps people's health. Preservation of water resources, removing the mentioned drugs from water improves the quality of water resources and gradually helps to preserve water resources. This action can help improve the sustainable use and proper management of water resources. Considering that drugs can act as important pollutants and need attention in water, removing them from water sources can have positive and valuable effects in preserving the environment and public health [24]. There have been numerous assessments of g-C_3N_4 for pollutant degradation and water disinfection up to this point. However, there are no comprehensive evaluations that focus on the most recent changes to g-C_3N_4 for the photodegradation of ciprofloxacin, acetaminophen (ACT), and carbamazepine (CBZ). In general, this review article examined the possibilities and g-C_3N_4 applications in the field of water treatment by focusing on the photodegradation of Acetaminophen, carbamazepine, and ciprofloxacin materials.

2. G-C_3N_4 Structure attributes and photocatalytic potential for water treatment

Basic Characteristics of g-C_3N_4 investigated of carbon nitride, particularly g-C_3N_4, dates back to 1834 [25]. Its synthesis by Wang and colleagues marked a significant breakthrough for applications, especially water splitting [26]. Because of its excellent physicochemical characteristics, g-C_3N_4 is the C_3N_4 allotrope that is the most stable under ambient conditions [27]. G-C_3N_4 possesses covalently bonded sp2-hybridized nitrogen and carbon atoms, forming a network of π-conjugated ring planes with a lattice structure akin to graphite [28]. The layers entail a hexagonal arrangement of nitrogen and carbon atoms, alternating seamlessly. The monolayer g-C_3N_4 network possesses a highly impressive theoretical specific surface area of up to 2500 m2g-1 [29]. This material exhibits a high theoretical specific surface area and comprises s-triazine (C3N3) and tri-s-triazine (C6N7) units formed through condensation processes [26, 30]. The C6N7 units show superior stability compared to C3N3 units, and the substance often displays surface defects with minimal hydrogen presence [31]. g-C_3N_4 also demonstrates remarkable thermal and chemical stability, enduring high temperatures and resisting decomposition in common solvents. The results of Thermogravimetric analysis (TGA) show that g-C_3N_4 demonstrates impressive heat endurance even in the presence of 100% oxygen [32]. Photocatalytic Capability of g-C_3N_4 under visible light exposure, g-C_3N_4 exhibits photocatalytic efficacy with valence band (VB) and conduction band (CB) positions at -1.1 eV and +1.6 eV, respectively [33]. Its optical absorption at 460 nm allows the capture of solar visible light, although slow hole-electron pair recombination. The bandgap of g-C_3N_4 can be altered, resulting in structural modifications and diverse packing conformations [34].

Rohit Kumar et al., developed a novel photocatalyst, KPCN/GO/ZnFe2O4, by modifying potassium and phosphorus co-doped graphitic carbon nitride (KPCN) with graphene oxide (GO) and forming a heterostructure with ZnFe2O4 through a hydrothermal process. This newly synthesized catalyst demonstrated impressive efficiency in degrading pollutants like tetracycline (TC), rhodamine B (RhB), and methylene

blue (MB) as well as removing chemical oxygen demand (COD) from actual wastewater. The KPCN/GO/ZnFe2O4 catalyst showed significantly improved degradation rates for tetracycline compared to unmodified graphitic carbon nitride, showcasing advancements achieved through doping, GO inclusion, and ZnFe2O4 incorporation. The photocatalytic process primarily relied on reactive species such as •OH and •O_2−, signifying the enhanced performance of the KPCN/GO/ZnFe2O4 catalyst due to improved light absorption, adsorption capacity, charge separation, and reusability [35]. This progress, achieved through doping, incorporation of graphene oxide (GO), and forming heterostructures, highlights the advancements made in improving light absorption, charge separation, and reusability for g-C_3N_4 -based materials [36].

2.1. Enhancing g-C_3N_4 photocatalysis

The pristine g-C_3N_4 in photocatalysis utilization is limited due to several factors. These limitations include its poor quantum efficiency, inadequate interfacial contact, high porosity, large dimension, fast photocarrier recombination, and difficulty dispersing into specific solvents, all of which contribute to poor filtration efficiency. These factors prevent the wide application of pristine g-C_3N_4 in photocatalysis [37]. Therefore, it is essential to adjust them into more diminutive structures in order to expand their pragmatic utilities. In accordance with the prerequisites, the process and concentration parameters are regulated correspondingly to generate diverse g-C_3N_4 morphologies. These minute configurations amplify the specific surface area and active sites, thus resulting in an increase in photocatalytic efficacy [38]. To reduce the pollution of the environment and improve large-scale waste water treatment, different morphologies are developed to quickly produce photocatalysts with outstanding photocatalytic activity [39].

Consequently, these endeavors have stimulated a shift towards innovative strategies focused on refining the morphology and structure of g-C_3N_4 to enhance its photocatalytic performance. By overcoming its inherent limitations through adjustments to more compact structures, scientists have effectively increased both specific surface area and active sites, resulting in a notable improvement in photocatalytic efficiency. This approach not only addresses the obstacles restricting the broad use of pristine g-C_3N_4 in photocatalysis but also significantly contributes to curbing environmental pollution and advancing large-scale wastewater treatment capabilities [40].

Gang Wang et al., developed a novel composite catalyst (g-C_3N_4 / NCDs/Ag) to degrade organic pollutants in water. By controlling electronic interactions and dual-doping with NCDs and Ag NPs, this catalyst showed enhanced electron transport and widened light absorption. It efficiently degraded various pollutants within 100 minutes under a xenon lamp, outperforming traditional g-C_3N_4 notably with specific contaminants like methyl orange and rhodamine B. Uniform distribution of NCDs and Ag NPs through g-C_3N_4 self-assembly enabled stable catalyst recycling. The primary active substance in the process was •O_2–, with •OH serving as a secondary contributor. This innovative double-doped g-C_3N_4 design holds promise for diverse applications [41].

2.1.1. G-C_3N_4 Synthesis insights

In the past ten years, g-C_3N_4 has become a well-known synthetic polymer in the realms of material science and chemistry, particularly in the subject of photocatalysis. This is because of its low cost, unique physicochemical properties, good stability, and ease of preparation, following its discovery in 2009 as a metal-free polymer semiconductor that produces H_2 by photocatalysis. C3N3 and C6N7 rings constitute the fundamental tectonic units of C_3N_4, which are widely regarded as its distinctive architecture [26]. Generally, g-C_3N_4 materials can be easily synthesized through heat condensation using small organic molecules as nitrogen-rich precursors, such as cyanimide and dicyanamide, urea, thiourea, and the tectonic units kind are largely dependent on response mechanisms. To gain a better understanding of the synthesis, Zhang et al. [42] conducted a study where they utilized either urea or thiourea as precursors for g-C_3N_4 production. Their findings revealed that the preparation process primarily consists of nucleophilic furthermore, polymerization, and polycondensation. The conversion of thiourea or urea molecules to melamine through condensation reactions was initially achieved, whereas dicyandiamide molecules underwent direct condensation to form melamine. Upon elevation of temperature, melamine underwent a rearrangement process to form tri-s-triazine units which were subsequently polymerized to produce g-C_3N_4. Melamine Thermal polymerization, cyanamide, dicyandiamide, urea, or thiourea at temperatures ranging from 450 to 550 °C is generally used to create C_3N_4 [43, 44]. In a similar manner, the production of polymeric g-C_3N_4 through the utilization of cyanamide was explored by [26], through the analysis of reaction intermediates at varying temperatures in order to earn a deeper the reaction mechanisms understanding and microscopic processes involved. Through the polycondensation of cyanamide molecules, melamine and dicyandiamide were formed at temperatures of approximately 234°C and 203°C, respectively, as noted by [45]. Then, it was found that all melamine-revelent intermediates were produced at a temperature of about 335°C and then were changed into basic tri-s-triazine rings at a temperature of about 390°C. Upon reaching a temperature of 520 °C, g-C_3N_4 was produced via the polymerization of the aforementioned fundamental units. However, the compound proved to be unstable and the structure gradually disintegrated beyond 600 °C, leading to the complete decomposition of g-C_3N_4 into smaller molecules, such as CO_2 and NH3, beyond 700 °C. In light of this, g-C_3N_4 samples that were derived from different precursors, temperature-rise paths, and thermolysis temperatures, were found to exhibit unique characteristics. Mo and coworkers found that the degree of light absorption and the g-C_3N_4 shrunk bandgap increased when the calcination temperature rose. [46]. The direct heating of melamine at 650°C resulted in the production of g-C_3N_4 with optimal photodegradation activity for methylene blue and 4-chlorophenol, together with exceptional stability. The reaction atmosphere, which includes Ar and H_2, NH3, and can produce disordered structures and defects, is yet another important element that intrinsic structures of g-C_3N_4 and affects the properties. For instance, the dicyandiamide thermal status under H_2 hydrogen led to the engineering of additional nitrogen vacancies [47]. NHx sites, on the other hand, increased the hydrogen bonding contact between layers and stopped tri-s-triazine rings from degrading on their own. This was because CO_2 promoted the growth of NHx sites [48]. Pretreatment of nitrogen-rich precursors is done to improve the g-C_3N_4 physicochemical properties before thermal annealing techniques, including protonation and sulfur-mediated synthesis. Improved photocatalytic behaviors are the consequence of controlling these reactive variables to produce the optimum level of condensation, a smaller band gap, and nanoarchitecture engineering [17].

Iltaf Khan et al., g-C_3N_4 nanosheets were synthesized using Eriobotrya japonica like a stabilizer and mediator . These bio-caped g-C_3N_4 nanosheets displayed enhanced properties such as strong adsorption, abundant organic functional groups, and activated surfaces. Capabilities, suitable for bisphenol A degradation and CO_2 conversion. The incorporation of LaFeO3 nanosheets via the SrO bridge further increased surface area, improved charge separation, and facilitated electron transportation. Compared to pure g-C_3N_4 nanosheets, the ultimate composite showed significant enhancements, improving CO_2 conversion by 8 times and bisphenol A degradation by 2.5 times. This research introduces an eco-friendly and efficient approach for designing green nanomaterials, supporting efforts towards net-zero carbon emissions and advancing carbon neutrality [49].

2.1.2. Designing advanced of g-C_3N_4 preparation technology

There has been a notable influx of nanomaterials based on g-C_3N_4, which have been deliberately designed and manufactured to surpass the constraints of pure or bulk g-C_3N_4 when applied. The methodologies employed for their synthesis prioritize attaining structural and morphological control in order to achieve desirable energy bands, fast charge transfer, and strong light absorption. In order to produce distinctive morphologies and organized porosity onto bulk g-C_3N_4, both soft and hard template approaches are preferred for the design of nanostructures. These include multidimensional nanoarchitecture, porous g-C_3N_4, hollow spheres, and more [50, 51]. The traditional method of using hard templates involves combining precursors with hard structure directing agents during pyrolysis processes, such as colloidal SiO_2 and mesoporous SiO_2 nanoparticles [50]. Subsequently, the templates are etched using F, NH4HF2, and various strong alkaline solutions to achieve the desired nanostructures. Zhang and coworkers, used colloidal SiO_2 (12 nm) and dicyandiamide like the template and precursor, respectively, to create mesoporous g-C_3N_4 [52]. In order to alter the structures, several precursor types and concentrations were used. It was demonstrated that g-C_3N_4's BET surface, which had an ideal weight ratio of 50 wt%, could increase with a drop in cyanamide. When exposed to visible light irradiation, the optimized sample's tetracycline removal rate showed the rate exceeded that of bulk g-C_3N_4 by 6.6 times. A variety of mesoporous silica templates, like SBA-16, SBA-15, KIT-6, and KCC-1, were used in addition to SiO_2 nanospheres to create well-ordered g-C_3N_4 structures [53]. The ordered g-C_3N_4 porous design considerably enhances the photocatalytic performance by enhancing mass transfer and expanding the reaction area. A more eco-friendly technique termed "greener" soft-template synthesis has been devised to

replace the usage of risky and expensive etchants like HF and NH4HF2. This method uses ionic liquids and amphiphilic block polymers as soft structure-directing agents to create g-C_3N_4 with a characteristic porous structure [51]. For example, Wang et al., [54] altered the g-C_3N_4 structure using dicyandiamide and a range of soft templates. These templates were made from amphiphilic block polymers such as P123, Brij30, Brij58, Triton X-100, F127, and Brij76 as well as nonionic and ionic surfactants like BmimDCNB, BmimCl, and mimPF6. It is a notable accomplishment that mesoporous g-C_3N_4 materials were created with remarkable porosity. Additionally, the employment of non-covalent bonding in supramolecular self-assemblage, a unique self-templating technique, enables the creation of stable and effectively designed materials without the need for external templates [54]. The final products are composed of the ordered molecular building blocks that are produced when monomers self-assemble through hydrogen bonding. As opposed to bulk g-C_3N_4, multi-dimensional g-C_3N_4 nanomaterials have been created in a variety of shapes and sizes, including 2D nanosheets, 1D nanotubes, quantum dots, and others [54]. Both the bottom-up and top-down approaches are frequently used in synthetic methods. Bulk g-C_3N_4 was fragmented into finely scattered and distinct nanostructures for the top-down approach with the help of external forces, particularly for its exfoliation into g-C_3N_4 nanosheets, such as liquid exfoliation ways, post-thermal oxidation etching method, etc. However, anisotropic bottom-up assembly necessitates certain organic molecules as well as a growing environment that includes diverse media, including structure-directing agents and required templates. At the moment, efforts are still being made to create and synthesize g-C_3N_4-based nanomaterials, producing g-C_3N_4 with various structures, morphologies, and sizes. This leads to the attainment of photocatalytic activity and superior optical characteristics [17].

Chellapandi Bhuvaneswari and Sundaram Ganesh Babu showed A highly robust ternary electrocatalyst, consisting of graphene-based CuS spheres on an exfoliated g-C_3N_4 sheet, has been developed using nanoarchitecture and surface engineering techniques. This electrocatalyst exhibits excellent electrochemical properties and was used to create a sensitive electrochemical sensor for detecting furazolidone (FZ). The sensor displayed a linear range from 0.1 to 336.4 μM, with a low limited detectability of 0.0108 μM, demonstrating a strong relationship between current and potential. Moreover, the composite showed remarkable electrocatalytic activity, selectivity against interfering compounds, and good reproducibility, stability, and repeatability, making it a promising platform for graphene-based materials in electrochemical FZ detection [55].

2.1.3. Advancements in Synthesis Techniques for g-C_3N_4 Nanocomposites

Over the past years, there has been a significant rise in the development of g-C_3N_4-based nanocomposites as potential photocatalysts for treating organic wastewater. Numerous synthesis techniques including sol-gel methodologies, hydrothermal and solvothermal have been explored to create versatile g-C_3N_4-based hybrids [53].

Among these methodologies, the sol-gel approach, a multi-step wet chemical process, is widely recognized for its suitability in producing nanomaterials due to cost-effectiveness and moderate reaction conditions [56]. This technique involves synthesizing a heterostructure by depositing metal nanoparticles on the semiconductor's surface, resulting in active constituents being deposited on g-C_3N_4. For instance, Li et al. fabricated g-C_3N_4/TiO_2 hybrids through an adjusted sol-gel pathway, creating a type II heterostructure to improve photoinduced electron separation and transfer [57]. Similarly, Chang et al. employed sol-gel techniques to produce C_3N_4/TiO_2 heterostructures with high BET surface areas and solid structures [58].

Additionally, G-C_3N_4-based nanocomposites have been synthesized using the hydrothermal method, which proves an effective approach and to be relativvely inexpensive. These structures typically exhibit high purity, increased crystallinity, and well-designed structures. Ji et al. utilized an in-situ hydrothermal synthesis method to decorate CdS onto g-C_3N_4, facilitating charge separation by locating the CdS nanoparticles near the g-C_3N_4 [50]. Similarly, Deng et al. developed SnS2 on g-C_3N_4, resulting in an evenly dispersed system with robust visible light-induced activity [59]. Furthermore, the solvothermal method is commonly employed to fabricate nanocomposites with distinctive morphologies. Reaction media, raw material selection, and solution conditions play essential roles in determining the catalysts' structures and activities [60]. Liang et al. utilized a solvothermal approach to design Bi2MoO6-gC_3N_4 heterostructures at various pH ranges, demonstrating superior photodegradation performance compared to single g-C_3N_4 and Bi2MoO6 for removing RhB [61]. Similarly, the ionic liquid 1-hexadecyl-3-methylimidazolium bromide was combined with Bi(NO3)3 in an EG/g-C_3N_4 solution by Xia et al., resulting in strong photodegradation efficiency for BPA and RhB [62]. Moreover, researchers have employed solvothermal techniques to enhance nanocomposite properties. Y. Zhang et al. successfully inserted Bi2MoO6 and Bi NPs into g-C_3N_4, achieving remarkable photodegradation efficiency and creating indirect Z-scheme heterojunctions and well hollow microspheres in g-C_3N_4/Bi2MoO6/Bi [63]. Additionally, S Meng loaded NiSx NPs as a cocatalyst onto g-C_3N_4, enhancing photocatalytic H_2 production Nanocomposites produced using the solvothermal method exhibit impeccable morphologies and distinctive inner structures, displaying superior catalytic performances under visible light. Optimizing synthesis parameters like reaction conditions and precursor concentrations is crucial for shaping nanocomposite morphology and improving photocatalytic efficacy. These adjustments impact properties like surface area and crystallinity, influencing the catalytic [64]. G-C_3N_4-based nanocomposite's performance in breaking down pollutants. Additionally, innovative techniques such as doping and surface modification enhance charge separation efficiency, boosting the overall photocatalytic activity.

These modifications refine optical and electronic properties, enabling better utilization of visible light for improved pollutant degradation [65].

Zeinab Talebzadeh et al, employed rapid ultrasonic treatment to fabricate $La_2SN_2O_7$/graphitic carbon nitride (LSO/CN) nanocomposites, using broccoli extract as a natural surfactant to control crystal nucleation and growth while preventing agglomeration. Varied experimental parameters allowed control over the nanocomposites' size and shape, assessed through diverse characterization techniques. The photocatalytic efficiency was evaluated by eliminating different dyes under UV light, and studying the impact of particle size, LSO: CN ratio, dye type, scavenger, and catalyst loading on catalytic efficiency. The research also delved into the potential photocatalytic mechanism underlying dye removal [66].

3. G-C_3N_4's photocatalytic mechanism

G-C_3N_4's photocatalytic activity involves light absorption, charge carrier generation and movement, redox reactions, and the breakdown of pollutants or hydrogen production, depending on the specific application and conditions [67, 68]. Utilizing photocatalysis, which offers potential for cost-efficiency and sustainable use represents an environmentally friendly approach for breaking down organic pollutants. However, creating photocatalysts with superior catalytic performance remains a considerable challenge in terms of their thoughtful design and production [69]. Light Absorption: g-C_3N_4 absorbs light (especially visible light), causing electrons to transition from the valence band to the conduction band, resulting in the creation electron-hole pairs [70]. Redox Reactions: Holes participate and photogenerated electrons in redox reactions. Holes can oxidize hydroxide ions or water to form highly responsive radicals such as hydroxyl radicals (•OH) or superoxide radicals (•O_2-) [71]. Formation of Active Species: Electrons in the conduction band can reduce oxygen to form reactive species like superoxide radicals (•O_2-) or react with hydrogen ions to generate hydrogen peroxide (H_2O_2) [72]. Charge Carrier Migration and Separation: Effective migration and separation of these charge carriers are crucial to prevent their recombination, thereby ensuring efficient catalytic activity [73]. Reaction with Pollutants: Photogenerated electrons and reactive species attack and break down organic pollutants adsorbed on the g-C_3N_4 surface, leading to their degradation into less harmful substances [74].

Hydrogen Evolution Reaction (HER): Under water's influence, g-C_3N_4 can also facilitate the generation of hydrogen gas by using photogenerated electrons to reduce protons from water [75].

Under the correct lighting circumstances, photogenerated electron-hole pairs can be used to explain the g-C_3N_4 photocatalytic activity. Reactive oxygen species (ROS) production and electron transfer are shown in Eqs (1)–(4) [76, 77]. The valence band (VB) electrons in g-C_3N_4 became excited and migrated from the conduction band (CB) to the surface, where they initiated a number of reactions. It is not possible to directly create hydroxyl radicals (•OH) via holes in H_2O and VB due to the negative VB potential being bigger than the typical H_2O/•OH and OH-/•OH redox potentials. The primary reactive chemicals assumed to be involved in the oxidation of organic pollutants are believed to be photogenerated holes, hydroxyl radicals, and superoxide anion radicals (•O_2 -) [33]. According to [78], the importance of hydroxyl radicals, hydrogen peroxide species, and superoxide anion radicals in photocatalytic disinfection cannot be emphasized. . These ROS have demonstrated effectiveness in reacting with cell membranes and cellular constituents,ultimately culminating in cellular demise [79].

(1) $g\text{-}C_3N_4 + light \rightarrow g\text{-}G_3N_4 (h^+ + e^-)$

(2) $g\text{-}C_3N_4 (e\text{-}) + O_2 \rightarrow g\text{-}C_3N_4{+}O^{-2}$

(3) $2\ g\text{-}G_3N (e^-) + O_2 + 2h+ \rightarrow 2\ g\text{-}GN_4 + H_2O_2$

(4) $H_2O_2 + g\text{-}G_3N_4 (e^-) \rightarrow g\text{-}G_3N_4 + .OH + 0H\text{-}$

Zuoyin Liu et al. investigated the g-C_3N_4/BiOI (001) photocatalytic mechanism using hybrid functional estimations based on first-principles theory. The interface exhibits a staggered band design with a built-in electric field from g-C_3N_4 to BiOI. Photo-generated electrons in BiOI's conduction bands combine again with holes in g-C_3N_4's valence bands due to the electric field and Coulomb interaction, forming a direct Z-scheme heterostructure. This separation of electrons and holes enhances their migration, leading to effective participation in redox reactions with water/pollutants, creating active species like hydroxyl radicals and superoxide ions. The larger difference in carrier effective masses in the g-C_3N_4/BiOI (001) heterostructure contributes to its superior photocatalytic activity observed in experiments, resolving certain experimental speculations and controversies [80].

3.1. Improvement of photocatalytic performance of g-C_3N_4

Enhancement of g-C_3N_4 photocatalytic capability involves enhancing its efficiency in utilizing light energy to drive catalytic reactions, Either for the degradation of the production or pollutants of valuable products. Several strategies can contribute to enhancing g-C_3N_4's photocatalytic performance inclined Modification of Structure, Doping, Surface Engineering, Heterojunction Formation, Optimization of Synthesis Parameters and Surface Defects and Active Sites [81-83]. Each of these approaches aims to address specific limitations or enhance the inherent properties of g-C_3N_4 to boost its effectiveness as a photocatalyst for environmental remediation or energy production applications [84].

3.1.1. Metal or non-metal doping

To enhance the efficiency of semiconductors with low conductivity, various materials, including metals and non-metals, are incorporated [85]. Transition Metals: Utilizing transition metals like Zr, W, Cu, Ag, and Fe as dopants for photocatalytic semiconductors has shown potential synergistic effects. For instance, Fe-doped g-C_3N_4 and Co-doped g-C_3N_4 exhibit enhanced performance in TOC removal in wastewater due to permonosulphate (PMS) activation [18]. Specific Metal Examples: The utilization of metals in elemental doping procedures, such as combining precursors with the template/metal salt solution during the doping process, has been observed. For example, Guo synthesized S and K-doped g-C_3N_4 by mixing KOH, (NH4)2SO4, and Sulphur (S) precursors with dicyanamide and melamine templates [86]. Metal doping in g-C_3N_4, such as Zr, Cu, Fe, or Co, has shown promise in activating persulphates or hydrogen peroxide, thereby enhancing the removal of total organic carbon (TOC) in wastewater treatment processes [87]. The incorporation of transition metals like Zr, W, Cu, Ag, and Fe, among others, as dopants in g-C_3N_4 demonstrate potential synergistic effects, accentuating their catalytic capabilities in various photocatalytic reactions [88, 89].

Non-Metal Doping: Non-Metallic Elements: Non-metallic elements including X, B, Ni, P, S, and O are used in semiconductor doping processes to maintain metal-free attributes and prevent irregular chemical state fluctuations resulting from metal ions' presence [90]. Specific Non-Metal Examples: Incorporating elements like sulfur, phosphorous, and oxygen into g-C_3N_4 through doping processes leads to alterations in electronic band structures, improved stability, enhanced photocatalytic activity, reduced bandgap energies, and increased light absorption [91-94]. Co-Doping Effects: Co-doping, such as S and K co-doped g-C_3N_4, has demonstrated significant reductions in the bandgap, allowing increased absorption of visible light. Co-doping is beneficial as it enhances photocarrier separation channels, ultimately improving the photocatalyt-

ic process [95].

Non-metallic elements like X, B, Ni, P, S, and O are utilized in semiconductor doping to maintain metal-free attributes while positively influencing the compound's chemical states, thereby preventing anomalous fluctuations due to the presence of metal ions [96].

Doping g-C_3N_4 with elements like sulfur, phosphorus, and oxygen has shown notable improvements in altering electronic band structures, enhancing long-term stability, and modulating the photocatalytic activity of the material [45].

Hao Zhang et al., discussed alkali metal (Li, Na, K, and Rb) doped g-C_3N_4 through high-temperature calcination and water bath heating. Both computational and experimental analyses were conducted to assess the photoelectric properties. Computational findings revealed that Rb-doped g-C_3N_4 exhibited significantly increased absorption spectra within the 500–1100 nm wavelength range, corroborating UV–vis spectrum results. Specifically, Rb-doped g-C_3N_4 demonstrated superior performance in CO_2 photo-reduction, generating CO at a rate exceeding three times higher than bulk g-C_3N_4. This research offers valuable insights for developing doped g-C_3N_4 materials applicable in, medical imaging, energy conversion, and environmental remediation [97].

3.1.2. Deposition of metals

An approach that is frequently used to improve the properties of semiconductor photocatalysts is metal deposition. This method involves the direct application of metals onto the surface of the target material through the use of heating techniques [94]. Deposition and doping are two distinct processes; the former involves the mere introduction of metals onto a surface, whereas doping is the replacement of specific atoms with dopants. In photocatalysis, the optoelectronic properties of catalysts can be improved by depositing noble metals onto their surfaces. However, this approach can be costly [95]. Noble metals are known to enable the development of robust electromagnetic fields as a result of local surface plasma resonance (LSPR), thereby photocatalytic reactions benefit from quicker and more efficient light absorption [98]. In addition, the formation of Schottky barriers at the catalyst interface enhances noble metals' ability to attract electrons. This prevents internal photocarrier recombination, produces an extra hole in place of the electron, and therefore improves photocatalytic efficiency [44]. To overcome these challenges, exploring non-precious metals for LSPR and optimizing modification techniques becomes crucial. TiN, known for its stable nature, wide-spectrum light absorption, and LSPR effect, has garnered considerable attention [99]. RhB was completely eliminated from g-C_3N_4 by placing the ideal quantity of silver NPs there by the reduction reaction of NaBH4 in about 60 minutes [100]. several techniques were utilized in the production of photocatalysts with varying shapes and sizes. These methods comprised deposition using auric chloride (AuCl4-), photoreduction, and thermal polymerization with melamine precursors. The catalyst has a much greater BET surface area, which is the cause of its enhanced stability, which in turn resulted in the remarkable photocatalytic activity exhibited against RhB [61], and methyl orange (MO) dyes [101]. Regarding cost considerations, non-precious metals have surfaced as a viable alternative and have been demonstrated to be effective counterparts [102]. A number of scholars endeavored to deposit non-precious metals onto the g-C_3N_4 structure through the incorporation of Cu and Bi metals, which facilitated a more expeditious separation of charge carriers and light absorption during the photocatalytic degradation process [102, 103].

Yuanyuan Liu et al., focused on environmentally friendly ways of producing hydrogen peroxide (H_2O_2) using photocatalysis. Non-metal elements (B, P, and S) were doped into g-C_3N_4 tubes (B-CNT, P-CNT, and S-CNT) through thermal polymerization and hydrothermal synthesis, significantly improving the yield of g-C_3N_4 tube materials. These doped photocatalysts demonstrated enhanced photocatalytic H_2O_2 production rates (42.31 μM min^{-1} for B-CNT, 24.95 μM min^{-1} for P-CNT, and 24.22 μM min^{-1} for S-CNT) compared to bulk CN (16.40 μM min^{-1}). The introduction of B, P, and S elements boosted photocatalytic activity by modifying and enhancing the separation of electron-hole carriers and electronic structures, showing promise for practical applications of CNT photocatalysts [104].

3.1.3. Heterojunction formulation

Combining semiconductors with additional semiconductor elements or compounds of equivalent energy levels to produce binary or ternary heterojunctions allows for the enhancement of charge carrier migration and makes charge separation easier. The mobility of the charges is increased in a heterojunction by the capacity of the electrons to move across the semiconductors while being influenced by an electric field. Many heterojunctions have been created to date, including Z-scheme (S-scheme), Schottky, p-n, Type-I, and Type-II heterojunctions. The enhancement of g-C_3N_4-based photocatalysts most frequently employed the Type II heterojunction mechanism. The S-scheme (Step-scheme) and Z-scheme heterojunctions have been used and developed for effective photocatalysis. In particular, the Type II heterojunction aids in the migration of electrons from the CB of semiconductor SC1 to the CB of semiconductor SC2, as well as holes from the VB of semiconductor SC2 to the CB of semiconductor SC1. The resulting free radical entities participate in active oxidation processes (AOP) and are made up of the leftover electron in SC1's CB and the hole in SC2's VB, respectively. The greater possibility of Coulombic repulsion of electrons during the migration of photogenerated electrons from one CB to another is blamed for the progressive decline in the preference for type II photocatalysts. A little degree of photocatalytic reduction capability was also demonstrated by the carriers after they were transferred to the semiconductor with low potential. As a result, the Z-scheme heterojunction pathway was developed, making it simpler for carriers in the CB of SC1 and VB of SC2 to take part in AOP by allowing the photogenerated e- in the CB of SC2 to undergo recombination with the VB of SC1 via interfacial transfer [105]. Another team of researchers developed the S-scheme heterojunction in order to boost photocatalysis efficiency by accelerating the recombination rate of holes under an inner electric area and low potency electron [106, 107]. The phenomenon of S-scheme heterojunction, which results in the inward bending of both semiconductors' band edges, is caused by the exact two semiconductors' alignment at their respective Fermi levels. As a result, the redox potential is favorable and there is effective photocatalytic activity, which facilitates the migration of electrons from the CB of the oxidation semiconductor to the reduction semiconductor VB [108]. In addition, it has been shown that the controlled production of a g-C_3N_4/BiPO4 Type II heterojunction using the ball milling approach results in a 97% breakdown of tetracycline. This extraordinary result can be attributed to the synthesized materials' high degree of the particular manner and crystallinity in which the interface formed [109]. In order to create heterojunctions, semiconductors are typically coupled with carbonaceous materials that contain conjugated structures, such as graphene oxides (GO), fullerenes, and carbon nanotubes(CNTs) [110]. By combining reduced graphene oxide (r-GO) and g-C_3N_4, a two-dimensional heterojunction hybrid was created that produced better interfacial conductivity and more charge carriers. They generate pairs of electrons and holes with relatively high redox potentials. The degradation efficacy of Z-scheme heterojunctions is superior to that of conventional heterojunctions. The Z-scheme heterojunction is a beneficial structure due to its ability to provide extended light absorption, separation efficiency, enhanced interfacial contact, improved oxidation capacity, and long-term stability [111]. Additionally, this structure has successfully overcome a number of drawbacks, such as the

avoidance of electrostatic attraction between electron and hole ions and a decline in the redox potentials of electron/hole pairs [112]. Z-scheme heterojunctions are characterized by the usage of mediators, such as noble metals, in the process of interfacial migration of electrons. Due to the semiconductors' close closeness to one another in the absence of these mediators, electron and charge transport occur at rapid rates [113].

Lu Wang et al. focused on creating a g-C_3N_4 and niobium pentoxide nanofibers (Nb_2O_5 NFs) heterojunction through an electrospinning method followed by calcination. Characterization confirmed a well-defined structure of g-C_3N_4/Nb_2O_5, where Nb_2O_5 NFs were tightly bound to g-C_3N_4 nanosheets. Analogized to individual g-C_3N_4 and Nb_2O_5 NFs, the resulting g-C_3N_4/Nb_2O_5 exhibited significantly improved photocatalytic performance in degrading phenol under visible light and rhodamine B. This enhanced performance stemmed from the synergistic effect between Nb2O5 NFs and g-C_3N_4 sheets, facilitating carrier transfer and preventing recombination, as supported by transient photocurrent responses and photoluminescence spectra. Active species trapping experiments identified superoxide radical anion ($\cdot O_2^-$) and hole (h^+) as major contributors to the photocatalytic process. The g-C_3N_4/Nb2O5 heterojunction, with its notable effectiveness and simple synthesis, holds promise for applications in treating organic pollutants and harnessing solar energy [114].

Jiawen Ren et al. focused on creating g-C_3N_4/NH_2-UiO-66 (Zr) heterojunction photocatalysts using an in-situ deposition and solvothermal method. These catalysts demonstrated highly efficient removal of hexavalent chromium (Cr (VI)) and simultaneous oxidation of tetracycline hydrochloride (TC-HCl). The results showed that the heterojunction structure had 1.86 times greater photocatalytic Cr (VI) removal efficiency compared to pure NH_2-UiO-66 (Zr) under visible light, with excellent stability and repeatability. Factors affecting the photocatalytic performance, such as Cr (VI) concentration and pH values, were investigated. Moreover, the heterojunction catalyst effectively removed pollutants in mixed solutions, achieving complete Cr (VI) reduction within 90 minutes under visible light while also enhancing TC-HCl oxidation. This study underscores the potential of heterojunction-structured photocatalysts for efficient wastewater purification [115].

3.1.4. Adjustment of the structure and regulations of defects

Formation defects are impurities that are introduced into the semiconductor matrix by the atom's subtraction or addition from the structural matrix. In particular, the ideal periodic organization of any given chemical is altered or impaired, which leads to the creation of defects. The presence of imperfections in semiconductors has significant implications in the realm of photocatalysis, as they can alter the composition and characteristics of a given compound [116]. Comparatively to crystalline structures, amorphous substances' chaotic atom arrangement reduces the possibility of defects. The effectiveness of photocatalysis can be improved by defects, according to an earlier study. The presence of vacancies within the semiconductor matrix can facilitate the formation of fresh active sites for the absorption of specific pollutants [117]. Until now, the majority of defect regulation mechanisms concerning g-C_3N_4 have been attained by means of generating nitrogen vacancies. This method proves to be convenient as the nitrogen vacancies can be readily created through the heating of g-C_3N_4 particles in an air/H_2 atmosphere [118]. Niu et al. [119], were able to create N_2 vacancies in the g-C_3N_4 matrix through the treatment of the substance under high temperatures in an air atmosphere. The resultant N-vacant g-C_3N_4 photocatalyst exhibited an increased absorption of visible light without any alteration to its structure conjugation and characteristics. Dong and colleagues [90], generated defective g-C_3N_4 material through the incorporation of carbon vacancies within its matrix. Subsequent irradiation with visible light led to the reduction of NO to N_2, with the defective catalyst exhibiting a faster pace of photocatalytic H_2 evolution in comparison to non-defective g-C_3N_4. In a separate study, Wu and co-workers [120], produced N-vacant g-C_3N_4 catalysts which resulted in a significant decrease in the bandgap, thereby facilitating fast charge transfer reactions. Ding and coworkers [121], conducted a process to modify the electronic structure of a material by eliminating N_2 atoms from terminal NHx groups. This procedure searched to make more active areas in the content more readily available. Exact N-void g-C_3N_4 catalysts have increased photocatalytic efficiency, charge separation effectiveness and light absorption. A comparable process for improving overall performance has also been found as structural tuning, which entails altering a material's morphology, structure, energy levels, and other features [122]. The catalysts made of 3D macroporous/mesoporous g-C_3N_4 possessed larger surface area and porosity, thereby demonstrating superior degradation performance. Chen and colleagues [123] used CaCO3 to create mesoporous g-C_3N_4 NPs and saw a speedy rise in the light absorption range from 460 nm to 800 nm causing a 12-fold increase in the rate of methylene blue (MB) degradation when compared to unmodified g-C_3N_4. With the discovery of porous honeycomb-structured g-C_3N_4, photodegradation activity was enhanced [124], and 3D g-C_3N_4 hollow bubbles [125]. Additionally, 2D and 1D g-C_3N_4 designs were modified to improve the multi-electron flow. Jin with his colleagues [126], through a two-step condensation method, created g-C_3N_4 nanotubes from melamine that resembled carbon nanotubes (CNTs). A six-fold increase in BET surface area and improved RhB removal potential were both seen in the synthesis of nanotubes. One method was used by Fan et al. [127] to create ultrafine g-C_3N_4 nanosheets with a thickness of 10 nm that closely resembled the graphite's sheet-like structure. The resultant nanosheets showed a significant five-fold increase in H_2 production, a remarkably high BET surface area of 211.2 m2/g, and the capacity to break down RhB in just 12 minutes.

Tao Yu et al., introduced a simple and environmentally friendly method to create nitrogen-defective g-C_3N_4 by employing urea and fumaric acid through thermal polymerization. This process induced nitrogen defects in the g-C_3N_4 structure, enhancing its photocatalytic action for hydrogen evolution by approximately 2.64 times compared to the original g-C_3N_4. These defects altered the band structure, leading to developed light absorption, efficient charge separation, and increased hydrogen evolution rates. The method's simplicity and eco-friendliness offer a promising approach for producing nitrogen-defective g-C_3N_4 with adjustable band structures [128].

Yingying Qin et al. explore a method to improve the photocatalytic hydrogen evolution of g-C_3N_4 by π-conjugation structure and integrating N defect engineering. The optimized DCN350 catalyst exhibited a remarkable hydrogen evolution rate of 1541.6 μmol g^{-1} h^{-1}, representing a 7.5-fold increase over pristine g-C_3N_4 (205.9 μmol g^{-1} h^{-1}). Through density functional theory (DFT) investigations and experiments, it was found that DCN350 with N defects not only broadened light absorption by reducing band gaps but also facilitated the hydrogen evolution reaction by acting as active sites. Additionally, the –C≡N functional group promoted charge spatial separation, enhancing the charge transfer and light absorption capacity of g-C_3N_4. This study sheds light on the role of structural defects in enhancing the photocatalytic hydrogen evolutionary activity [129].

4. G-C_3N_4 for pharmaceutical removal from water

The application of photocatalytic oxidation processes for eliminating pharmaceutical drugs from wastewater is regarded as an appealing and eco-friendly method [16]. G-C_3N_4 has appeared as a promising photoelectrocatalyst for water treatment. Researchers are exploring advanced oxidation processes (AOPs), particularly photoelectrocatalytic (PEC) systems, to develop sustainable methods for eliminating persistent con-

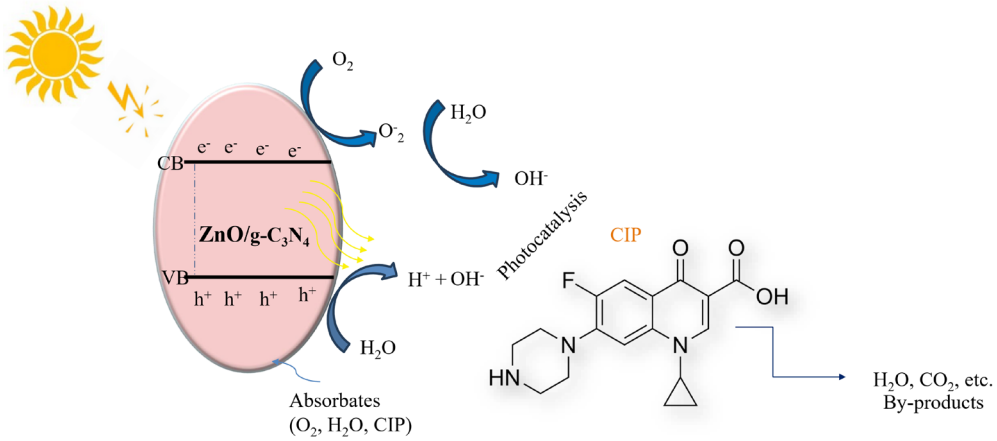

Fig. 1. Photodegradation of CIP under solar light-assisted ZnO/g-C_3N_4.

taminants from urban wastewater treatment plant effluents [130]. The utilization of g-C_3N_4 in pharmaceutical removal from water highlights its potential to address water pollution challenges caused by the presence of pharmaceutical residues [131]. Ciprofloxacin, acetaminophen, and carbamazepine are commonly found pharmaceuticals in water, undergoing photodegradation to break down their structures into less harmful substances when exposed to light, particularly under the influence of g-C_3N_4, a photocatalyst [132]. This catalyst generates electron-hole pairs upon light exposure, initiating redox reactions with this pharmaceutical [133]. This catalyst generates electron-hole pairs upon light exposure, initiating redox reactions with these pharmaceuticals. The adsorption of these compounds onto g-C_3N_4's surface leads to highly reactive species formation, such as hydroxyl radicals (•OH), which break down the molecular structures of these pharmaceuticals through oxidation-reduction reactions [134].

This degradation process facilitated by g-C_3N_4's photocatalytic activity aids in reducing or removing these pharmaceutical pollutants from water bodies [68]. Photocatalytic degradation of pharmaceuticals by different materials under varied light sources (summarized in Table 1).

4.1. Photodegradation of Ciprofloxacin

Ciprofloxacin (CIP), a widely used antibiotic belonging to the second-generation quinolone category, is prevalent in wastewater due to its limited breakdown through metabolic means. A significant portion of CIP is excreted unchanged and remains persistent in municipal wastewa-

Table 1.
Photocatalytic Degradation of Pharmaceuticals by Different Materials under Varied Light Sources - Summary of Main Results

Material	Pharmaceutical	Light source	Main results	Ref.
Boron-doped and nitrogen-deficient g-C_3N_4 (BNCN)	Acetaminophen	Visible light	100% in 30 min	[178]
TiO_2/g-C_3N_4-PS (persulfate)	Acetaminophen	Visible light	Almost completely degraded in 30 min	[179]
g-C_3N_4 nanosheets	Acetaminophen	Solar light	99% in one hour	[180]
g-C_3N_4@TiO_2 (gT), g-C_3N_4@TiO_2@ZnO (gTZ)	Acetaminophen	Visible light	For gT 70.6% and gTZ 92.4%	[179]
$CoFe_2O_4$/mpg-C_3N_4	Acetaminophen	UV light	100% in 25 min	[181]
BiOCl/g-C_3N_4 (BOC/CN)	Carbamazepine	Solar light	49% 240 min	[182]
g-C_3N_4/TiO_2	Carbamazepine	UVA light	71.41% in 360 min	[15]
C_3N_4@CuS	Carbamazepine	Visible light	98.5% in 5h	[183]
carbon-doped supramolecule-based g-C_3N_4/TiO_2	Carbamazepine	LED lamp	99.77% in 6h	[150]
Heterojunction of (P, S) co-doped g-C_3N_4 and 2D TiO_2	Carbamazepine	Solar light	100 % in less than 30 min	[137]
g-C_3N_4/Ag_3PO_4/Chitosan	Ciprofloxacin	Visible light	90.34% in 60 min	[184]
$CoFe_2O_4$/g-C_3N_4	Ciprofloxacin	Visible light	97% in 60min	[185]
ZnO/g-C_3N_4	Ciprofloxacin	Visible light	93.8% under pH 8	[13]
C_3N_4/Bp/MoS_2	Ciprofloxacin	Visible light	over 99% in 60 min	[186]
CeO_2/g-C_3N_4	Ciprofloxacin	Visible light	96.3% in 100 min	[187]

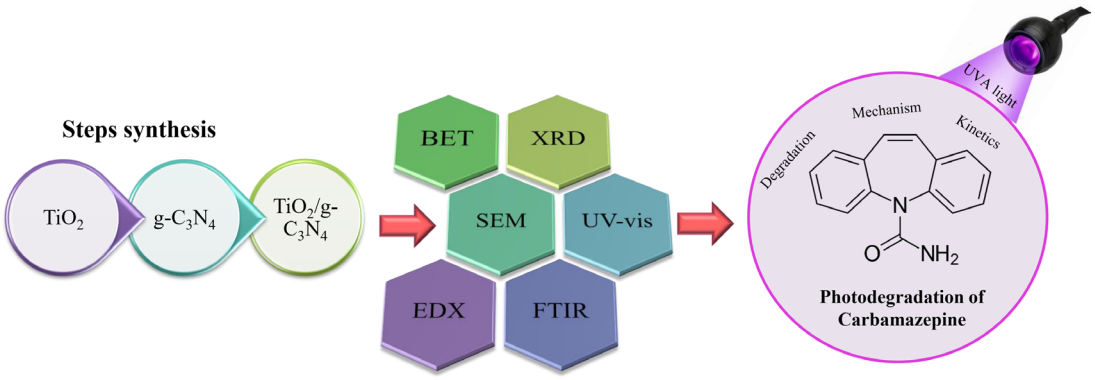

Fig. 2. Photodegradation of ACT for water remediation.

Characterization of Photocatalyst

ter [135]. Despite being discharged into the environment, CIP exhibits resistance to biodegradation in traditional wastewater treatment plants, leading to its detection in aquatic environments globally [136, 137]. This persistence poses risks like the development of bacterial medication resistance and toxicity to probiotics, necessitating effective removal techniques [138]. Photocatalysis offers a promising method for eliminating antibiotic residues from water [139, 140]. Studies have demonstrated the efficacy of various photocatalysts, such as Z-scheme nanocomposites of TiO_2/g-C_3N_4 and nitrogen-deficient g-C_3N_4 with carbon dots (C-dot@ND-g-C_3N_4) in CIP degradation [141, 142]. These photocatalysts exhibited remarkable degradation rates under simulated sun irradiation and visible light, showing significant improvement over commercial TiO_2 powder or g-C_3N_4 alone [143]. Mechanistic studies revealed the involvement of hydroxyl radicals and superoxide in the breakdown of CIP, with electron-hole pair separation, nitrogen defects, and carbon dots enhancing visible light absorption [142]. Additionally, heterojunction photocatalysts, such as Sm-doped g-C_3N_4/Ti3C2 MXene (SCN/MX) and g-C_3N_4/RGO/WO3, showcased enhanced charge separation and electron mobility [144, 145]. The reduced graphene oxide (RGO) incorporation as an electron mediator significantly improved the overall performance of the photocatalysts, leading to increased CIP degradation efficiency under visible light exposure [146]. Photocatalysis stands as a promising technique for eliminating antibiotic residues from water [147, 148]. Regarding to photocatalytic Removal Efforts Research has explored various approaches leveraging different photocatalysts to degrade CIP effectively [149]. For instance, Hu et al. developed a Z-scheme nanocomposite of 1D/2D TiO_2 nanorod/g-C_3N_4 nanosheet, demonstrating a 93.4% degradation rate for CIP within 60 minutes [150]. Zhang et al. introduced a green photocatalyst, C-dot@Nitrogen Deficient g-C_3N_4, which showed a 3.5-fold enhanced efficacy in CIP removal under visible light [151]. related to advancements in photocatalyst development Studies by Yu et al. introduced a heterojunction of Sm-doped g-C_3N_4/Ti3C2 MXene (SCN/MX), exhibiting over 99% photodegradation efficiency for CIP in the presence of visible light [152, 153]. Similarly, Lu et al. utilized a photoreduction technique to create the Z-scheme photocatalyst g-C_3N_4/RGO/WO3, indicating superior enhanced performance and charge separation in CIP degradation [154]. Doan Van Thuan et al. focused on employing a ZnO-modified g-C_3N_4 photocatalyst to degrade Ciprofloxacin (CIP) antibiotic compounds in water. The ZnO/g-C_3N_4 catalyst demonstrated a significant removal efficiency of 93.8% for CIP at pH 8.0. Increasing the catalyst amount improved pollutant degradation, achieving complete oxidation of low concentrations (1 mg L^{-1}) of CIP. At higher concentrations (20 mg L^{-1}), around a 13% decrease in removal efficiency was observed. The doped ZnO/g-C_3N_4 catalyst degraded CIP 4.9 times faster than undoped g-C_3N_4 and displayed strong reusability with 89.8% efficiency after 3 cycles. Active radical species like ·OH, ·O_2−, and h+ were identified as crucial in the degradation process. Additionally, the study proposed a mechanism detailing the degradation of CIP using visible light-assisted ZnO/g-C_3N_4 [13] (mentioned in Figure 1). Kang Hu et al., developed a Z-scheme nanocomposite using 1D/2D TiO_2 nanorods and g-C_3N_4 nanosheets, aiming for CIP-efficient photocatalytic degradation in water treatment. Achieving 93.4% CIP degradation in 60 minutes, the nanocomposite had optimal conditions with 30% g-C_3N_4, 15 µmol L^{-1} CIP concentration, and pH 6.3. The study systematically explored catalyst effects, and pH on degradation and CIP concentrations, fitting a pseudo-first-order kinetic model for CIP concentrations above 10 µmol L^{-1}. Under simulated sunlight, this nanocomposite exhibited 2.3 and 7.5 times higher CIP photodegradation rates compared to commercial TiO_2 powder and g-C_3N_4 nanosheets, respectively. Further investigations unveiled degradation kinetics, and mechanisms, and proposed three CIP degradation pathways, highlighting the role of h+ and ĔOH through electron spin resonance (ESR) technique and scavenging experiments. This research may offer an effective approach for eliminating various antibiotics in water treatment processes [155].

4.2. Photodegradation of Acetaminophen (ACT)

ACT, a prominent pharmaceutical compound, underwent photodegradation studies employing advanced photocatalysts in various experiments [156]. The photodegradation of acetaminophen offers several benefits, such as Environmental Impact, Water Treatment, Reduced Toxicity, and Public Health [157]. ACT photodegradation can be achieved through various techniques including Photocatalyst, UV Irradiation, Advanced Oxidation Processes (AOPs), Heterogeneous Photocatalytic Systems, and Hybrid Systems [158, 159]. Each technique offers distinct advantages in terms of efficiency, applicability, and degradation rates based on factors like catalyst type, light source, reaction conditions, and the concentration of acetaminophen in the system [157, 158]. Li et al., produced g-C_3N_4-CdS/Bi4O5I2 composites that demonstrated exceptional photocatalytic efficiency and stability for paracetamol degradation. The ternary heterojunctions facilitated enhanced charge transfer pathways, significantly boosting performance and stability, with the optimal sample exhibiting significantly higher degradation rates compared to individual components [160]. Moradi et al., developed TiO_2/graphene/g-C_3N_4 (TGCN), an efficient Z-type photocatalyst, by incorporating graphene as an electron mediator, enhancing degradation performance under simulated solar light. The study elucidated the enhanced band gap placement and charge separation mechanisms, leading to the efficient destruction of ACM under specific irradiation conditions [161].

Gupta et al., investigated the g-C_3N_4/PS system, demonstrating improved photocatalytic breakdown of ACT using hydrothermally treated g-C_3N_4 illuminated by 400 nm LEDs (HT-g-C_3N_4/PS system). They highlighted the superior charge transfer and photoelectron-hole separation properties of HT-g-C_3N_4, outperforming g-C_3N_4 in ACT degradation

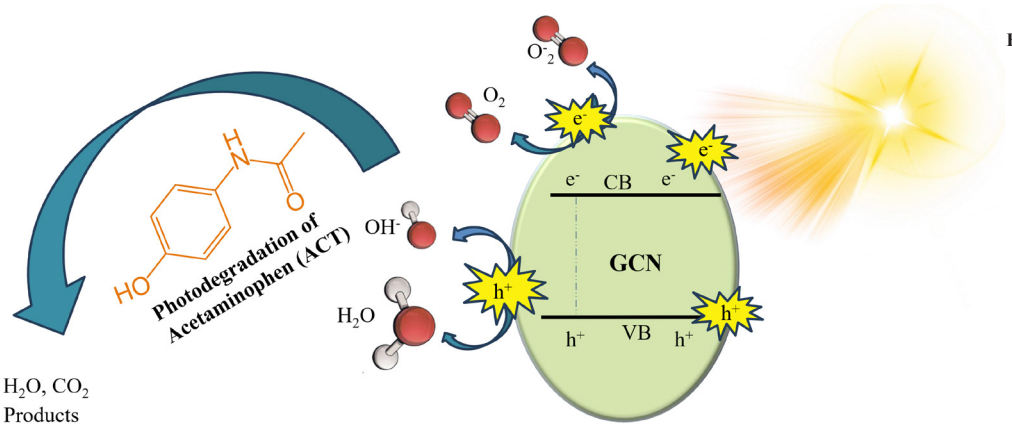

Fig. 3. Photodegration of Carbamazephin under UVA light.

under different conditions [162].

The comprehensive analysis of these studies evaluated the degradation kinetics, by-product identification, and potential applications in treating pharmaceutical pollutants in water resources [163]. Some findings presented diverse photocatalytic materials, elucidating their efficiencies, charge transfer mechanisms, and enhanced degradation capabilities, paving the way for promising solutions in water treatment [164, 165]. Photodegration of ACT for water remediation is shown in figure 2.

Elvana Cako et al., developed a new photocatalyst by combining phosphorus and sulfur co-doped g-C_3N_4 with 2D TiO_2 for solar-driven degradation of pharmaceutical pollutants. This composite demonstrated impressive photocatalytic activity, achieving almost complete degradation of carbamazepine (CBZ) within 30 minutes and complete removal of acetaminophen (ACT) in 60 minutes under simulated solar light. The composite showed excellent synergy in degrading CBZ and ACT, removing 76% and 40% of total organic carbon (TOC) respectively. Reactive oxygen species like hydroxyl radicals and superoxide played vital roles in the degradation process. The composite's structure effectively separated charge carriers, and its stability across multiple degradation cycles highlights its potential for environmental applications. They introduced a highly effective and stable photocatalyst for breaking down pharmaceutical pollutants, showcasing promising applications in environmental remediation [137].

4.3. Photodegradation of Carbamazepine

Carbamazepine is a pharmaceutical compound primarily used to treat epilepsy, bipolar disorder, and certain neuralgia pains [166]. Its photodegradation involves subjecting the compound to light-induced chemical reactions that break down its molecular structure [167]. The benefits of carbamazepine photodegradation include reducing its environmental impact and toxicity. Photodegradation can convert the compound into less harmful substances, aiding in its removal from water bodies or treatment processes [168, 169]. Various methods are employed for carbamazepine photodegradation, such as photocatalysis using semiconductor materials like TiO_2, ZnO, or graphene-based catalysts [170]. Advanced oxidation processes (AOPs), involving UV irradiation or the addition of hydrogen peroxide or ozone, are also effective in degrading carbamazepine [171]. These techniques harness light or reactive oxygen species to break down the compound into smaller, less harmful molecules [170, 172]. Zhou et al., developed a composite material using g-C_3N_4 nanosheets and CoCeOx nanospheres derived from MOF, showcasing abundant active sites, a compact interface, and a highly specific surface. This material demonstrated remarkable hydrogen generation efficiency of 1050 mol g-1 h-1 and exhibited significant carbamazepine degradation (97% within an hour at 0.05 min-1 rate) when assisted by PDS. The degradation products and pathways of carbamazepine were proposed through mass spectrometry and DFT calculations [136].

Gan et al.'s research explored the interaction between Fe2O3@g-C_3N_4 (FCN) and persulfate/sulfite in the breakdown of carbamazepine (CBZ). It revealed distinct roles of Fe2O3 in FCN for activating S(IV) and PS. In FCN/PS/vis and FCN/S(IV)/vis systems, the roles and contributions of Fe_2O_3 varied significantly, impacting CBZ elimination based on pH and catalyst charge [173].

Xu et al., produced ternary graphitic carbon nitride/zinc tetra carboxy phthalocyanine/graphene quantum dots (g-C_3N_4/ZnTcPc/GQDs). GQDs addition to g-C_3N_4/ZnTcPc/0.1GQDs caused the C-NH_2 peak to move from 286.0 eV to 285.7 eV and enhanced the C-C peak relative to the C-NH_2 peak, according to X-ray photoelectron spectroscopy (XPS) spectra. Under solar light irradiation, the g-C_3N_4/ZnTcPc/0.1GQDs composites showed improved photocatalytic activity. Notably, g-C_3N_4/ZnTcPc/0.1GQDs showed improved photocatalytic performance, removing carbamazepine in 180 minutes and sulfaquinoxaline sodium in 40 minutes, respectively, with removal rates of 63% and 59%. In-depth research has been done on the use of the peroxymonosulfate-based AOP as an effective method for the organic contaminants degradation in wastewater [174].

Yang et al., reported on a new 3D hierarchical heterojunction made of protonated g-C_3N_4/BiOBr, demonstrating high photocatalytic effectiveness for CBZ removal under simulated solar light. The study delved into operational variables like initial solution pH, photocatalyst dosage, and coexisting inorganic anions, attributing enhanced catalytic performance to efficient charge separation at the interface between phases [175].

Mei et al., introduced a novel method using potassium persulfate (KPS) as an oxidizing agent to create metal-free carboxyl-modified g-C_3N_4. This method efficiently activated PMS for CBZ degradation under sunlight, achieving approximately 100% CBZ removal within 20 minutes, without the use of strong acids or organic solvents [176].

Abdoulaye Kane et al., synthesized a UVA light-driven g-C_3N_4/TiO_2 photocatalyst for degrading Carbamazepine (CBZ) in water. The composite structures and TiO_2, g-C_3N_4, were examined utilizing various techniques like UV–vis DRS, SEM with EDX, BET nitrogen adsorption–desorption isotherm, Raman Spectroscopy, and XRD . The developed composites (10%g-C_3N_4/TiO_2 and 30%g-C_3N_4/TiO_2) exhibited band gaps of 2.97 and 2.78 eV, respectively, and specific surface areas of 80.64 and 59.67 m2/g. Photodegradation studies revealed that the 10%g-C_3N_4/TiO_2 composite eliminated 71.41% of CBZ with 30.38% mineralization yield within 360 minutes of UVA irradiation under optimal conditions (10 ppm initial CBZ concentration and 0.1 g of 10%g-C_3N_4/TiO_2 loading). The degradation kinetics almost followed a First-order kinetic model, showing a high reaction rate constant of 0.0034 min^{-1} for the 10%g-C_3N_4/TiO_2 composite. is exhibited the synthesized g-C_3N_4/TiO_2 photocatalyst efficiency under UVA light for degrading CBZ, highlighting its potential application in water treatment processes [15]. Photodegration of Carbamazephin under UVA light illustrate in Figure 3.

Zihang Cheng et al., focused on synthesizing g-C_3N_4 enriched with tri-s-triazine groups to activate peroxymonosulfate (PMS) under visible light, termed the Vis/g-C_3N_4/PMS process, for degrading the persistent micropollutant carbamazepine (CBZ). This process raised the degradation rate of CBZ by 2 times compared to g-C_3N_4 alone under visible light, mainly due to the generation of HOradical dot and SO4radical dot– from PMS activation. It was observed that the enhanced degradation was not a result of improved charge separation in g-C_3N_4 because of PMS attendance. The Vis/g-C_3N_4/PMS process exhibited insensitivity to dissolved bicarbonate concentrations and oxygen, and chloride functioned effectively across a wide pH range from 6.0 to 10.0 and showed less susceptibility to high natural organic matter concentrations compared to other treatment processes like UV/TiO_2 and UV/chlorine. Furthermore, the g-C_3N_4 photocatalytic activity remained stable over five reuse cycles. These characteristics render the Vis/g-C_3N_4/PMS process practically relevant and applicable for degrading micropollutants in various water sources using natural sunlight or more efficient visible light LEDs [177].

5. Conclusions and future perspectives

In conclusion, the remarkable efficiency and cost-effectiveness of g-C_3N_4-based materials in pharmaceutical photodegradation present a compelling approach for water treatment. This review affirms the capability of g-C_3N_4-based materials to efficiently degrade persistent and emerging pollutants like Ciprofloxacin, Acetaminophen, and Carbamazepine in water. However, advancing the optimization of material properties and operational conditions is essential to maximize efficacy. To address the challenges associated with eliminating emerging contaminants from water resources, the development of highly effective and economically feasible photocatalysts is imperative. Prioritizing sustainable synthesis techniques for g-C_3N_4-based materials and evaluating the potential toxicity and environmental impact of generated by-products during photocatalytic degradation is crucial. This emphasizes the pivotal role of science and technology in tackling environmental challenges and underscores the ongoing need for research and development to devise efficient water treatment methodologies.

Acknowledgments

The authors received no financial support for the research, author-ship and/or publication of this article.

Conflict of interest

The authors declare that there is no conflict of interest.

REFERENCES

[1] J. Yu, M. Jaroniec, C. Jiang, Surface science of photocatalysis, Academic Press 2020.
[2] C. Bie, H. Yu, B. Cheng, W. Ho, J. Fan, J. Yu, Design, fabrication, and mechanism of nitrogen-doped graphene-based photocatalyst, Advanced Materials 33(9) (2021) 2003521.
[3] O.K. Dalrymple, E. Stefanakos, M.A. Trotz, D.Y. Goswami, A review of the mechanisms and modeling of photocatalytic disinfection, Applied Catalysis B: Environmental 98(1-2) (2010) 27-38.
[4] L. Zhang, X. Zhou, S. Liu, H. Liu, S. Zhu, Y. Mao, Q. Yang, S. Zhu, C. Zhang, T. Wang, C. Wang, Two birds, one stone: Rational design of Bi-MOF/g-C_3N_4 photocatalyst for effective nitrogen fixation and pollutants degradation, Journal of Cleaner Production 425 (2023) 138912.
[5] R.R. Ikreedeegh, M. Tahir, A critical review in recent developments of metal-organic-frameworks (MOFs) with band engineering alteration for photocatalytic CO_2 reduction to solar fuels, Journal of CO_2 Utilization 43 (2021) 101381.
[6] A. Meng, L. Zhang, B. Cheng, J. Yu, Dual cocatalysts in TiO_2 photocatalysis, Advanced Materials 31(30) (2019) 1807660.
[7] T. Di, Q. Xu, W. Ho, H. Tang, Q. Xiang, J. Yu, Review on metal sulphide-based Z-scheme photocatalysts, ChemCatChem 11(5) (2019) 1394-1411.
[8] C. Cheng, B. He, J. Fan, B. Cheng, S. Cao, J. Yu, An inorganic/organic S-scheme heterojunction H_2-production photocatalyst and its charge transfer mechanism, Advanced Materials 33(22) (2021) 2100317.
[9] P. Xia, M. Antonietti, B. Zhu, T. Heil, J. Yu, S. Cao, Designing defective crystalline carbon nitride to enable selective CO_2 photoreduction in the gas phase, Advanced Functional Materials 29(15) (2019) 1900093.
[10] Y. Yang, X. Li, C. Zhou, W. Xiong, G. Zeng, D. Huang, C. Zhang, W. Wang, B. Song, X. Tang, X. Li, H. Guo, Recent advances in application of graphitic carbon nitride-based catalysts for degrading organic contaminants in water through advanced oxidation processes beyond photocatalysis: A critical review, Water Research 184 (2020) 116200.
[11] H.A. Bicalho, J.L. Lopez, I. Binatti, P.F.R. Batista, J.D. Ardisson, R.R. Resende, E. Lorençon, Facile synthesis of highly dispersed Fe(II)-doped g-C_3N_4 and its application in Fenton-like catalysis, Molecular Catalysis 435 (2017) 156-165.
[12] C. Chen, M. Xie, L. Kong, W. Lu, Z. Feng, J. Zhan, Mn_3O_4 nanodots loaded g-C_3N_4 nanosheets for catalytic membrane degradation of organic contaminants, Journal of Hazardous Materials 390 (2020) 122146.
[13] D. Van Thuan, T.B.H. Nguyen, T.H. Pham, J. Kim, T.T. Hien Chu, M.V. Nguyen, K.D. Nguyen, W.A. Al-onazi, M.S. Elshikh, Photodegradation of ciprofloxacin antibiotic in water by using ZnO-doped g-C_3N_4 photocatalyst, Chemosphere 308 (2022) 136408.
[14] J. Fan, H. Qin, S. Jiang, Mn-doped g-C_3N_4 composite to activate peroxymonosulfate for acetaminophen degradation: The role of superoxide anion and singlet oxygen, Chemical Engineering Journal 359 (2019) 723-732.
[15] A. Kane, L. Chafiq, S. Dalhatou, P. Bonnet, M. Nasr, N. Gaillard, J.M.D. Dikdim, G. Monier, A.A. Assadi, H. Zeghioud, g-C_3N_4/TiO_2 S-scheme heterojunction photocatalyst with enhanced photocatalytic Carbamazepine degradation and mineralization, Journal of Photochemistry and Photobiology A: Chemistry 430 (2022) 113971.
[16] N.Q. Thang, A. Sabbah, L.-C. Chen, K.-H. Chen, C.M. Thi, P. Van Viet, High-efficient photocatalytic degradation of commercial drugs for pharmaceutical wastewater treatment prospects: a case study of Ag/g-C_3N_4/ZnO nanocomposite materials, Chemosphere 282 (2021) 130971.
[17] Z. Chen, S. Zhang, Y. Liu, N.S. Alharbi, S.O. Rabah, S. Wang, X. Wang, Synthesis and fabrication of g-C_3N_4-based materials and their application in elimination of pollutants, Science of The Total Environment 731 (2020) 139054.
[18] M. Raaja Rajeshwari, S. Kokilavani, S. Sudheer Khan, Recent developments in architecturing the g-C_3N_4 based nanostructured photocatalysts: Synthesis, modifications and applications in water treatment, Chemosphere 291 (2022) 132735.
[19] M. Ahmaruzzaman, S.R. Mishra, Photocatalytic performance of g-C_3N_4 based nanocomposites for effective degradation/removal of dyes from water and wastewater, Materials Research Bulletin 143 (2021) 111417.
[20] B. Zhu, B. Cheng, J. Fan, W. Ho, J. Yu, g-C_3N_4-based 2D/2D composite heterojunction photocatalyst, Small Structures 2(12) (2021) 2100086.
[21] M. Zhang, Y. Yang, X. An, L.-a. Hou, A critical review of g-C_3N_4-based photocatalytic membrane for water purification, Chemical Engineering Journal 412 (2021) 128663.
[22] A. Smýkalová, B. Sokolová, K. Foniok, V. Matějka, P. Praus, Photocatalytic Degradation of Selected Pharmaceuticals Using g-C_3N_4 and TiO_2 Nanomaterials, Nanomaterials 9(9) (2019) 1194.
[23] D. Fatta-Kassinos, S. Meric, A. Nikolaou, Pharmaceutical residues in environmental waters and wastewater: current state of knowledge and future research, Analytical and Bioanalytical Chemistry 399(1) (2011) 251-275.
[24] A.M.E. Khalil, F.A. Memon, T.A. Tabish, D. Salmon, S. Zhang, D. Butler, Nanostructured porous graphene for efficient removal of emerging contaminants (pharmaceuticals) from water, Chemical Engineering Journal 398 (2020) 125440.
[25] Y. Gong, M. Li, H. Li, Y. Wang, Graphitic carbon nitride polymers: promising catalysts or catalyst supports for heterogeneous oxidation and hydrogenation, Green Chemistry 17(2) (2015) 715-736.
[26] X. Wang, K. Maeda, A. Thomas, K. Takanabe, G. Xin, J.M. Carlsson, K. Domen, M. Antonietti, A metal-free polymeric photocatalyst for hydrogen production from water under visible light, Nature materials 8(1) (2009) 76-80.
[27] D.M. Teter, R.J. Hemley, Low-compressibility carbon nitrides, Science 271(5245) (1996) 53-55.
[28] A. Thomas, A. Fischer, F. Goettmann, M. Antonietti, J.-O. Müller, R. Schlögl, J.M. Carlsson, Graphitic carbon nitride materials: variation of structure and morphology and their use as metal-free catalysts, Journal of Materials chemistry A 18(41) (2008) 4893-4908.
[29] T. Sano, S. Tsutsui, K. Koike, T. Hirakawa, Y. Teramoto, N. Negishi, K. Takeuchi, Activation of graphitic carbon nitride (gC_3N_4) by alkaline hydrother-

mal treatment for photocatalytic NO oxidation in gas phase, Journal of Materials Chemistry A 1(21) (2013) 6489-6496.
[30] K. Yu, X. Hu, K. Yao, P. Luo, X. Wang, H. Wang, Preparation of an ultrathin 2D/2D rGO/gC_3N_4 nanocomposite with enhanced visible-light-driven photocatalytic performance, RSC advances 7(58) (2017) 36793-36799.
[31] X. Bai, L. Wang, R. Zong, Y. Zhu, Photocatalytic activity enhanced via g-C_3N_4 nanoplates to nanorods, The Journal of Physical Chemistry C 117(19) (2013) 9952-9961.
[32] J. Zhu, Y. Wei, W. Chen, Z. Zhao, A. Thomas, Graphitic carbon nitride as a metal-free catalyst for NO decomposition, Chemical communications 46(37) (2010) 6965-6967.
[33] S. Cao, J. Low, J. Yu, M. Jaroniec, Polymeric photocatalysts based on graphitic carbon nitride, Advanced Materials 27(13) (2015) 2150-2176.
[34] X. Li, G. Huang, X. Chen, J. Huang, M. Li, J. Yin, Y. Liang, Y. Yao, Y. Li, A review on graphitic carbon nitride (g-C_3N_4) based hybrid membranes for water and wastewater treatment, Science of The Total Environment 792 (2021) 148462.
[35] R. Kumar, A. Sudhaik, P. Raizada, V.-H. Nguyen, Q. Van Le, T. Ahamad, S. Thakur, C.M. Hussain, P. Singh, Integrating K and P co-doped g-C_3N_4 with $ZnFe_2O_4$ and graphene oxide for S-scheme-based enhanced adsorption coupled photocatalytic real wastewater treatment, Chemosphere 337 (2023) 139267.
[36] Q. Wang, Y. Li, F. Huang, S. Song, G. Ai, X. Xin, B. Zhao, Y. Zheng, Z. Zhang, Recent advances in g-C_3N_4-based materials and their application in energy and environmental sustainability, Molecules 28(1) (2023) 432.
[37] N.F. Moreira, M.J. Sampaio, A.R. Ribeiro, C.G. Silva, J.L. Faria, A.M. Silva, Metal-free g-C_3N_4 photocatalysis of organic micropollutants in urban wastewater under visible light, Applied Catalysis B: Environmental 248 (2019) 184-192.
[38] J. Pan, Y. Liu, W. Ou, S. Li, H. Li, J. Wang, C. Song, Y. Zheng, C. Li, The photocatalytic hydrogen evolution enhancement of the MoS_2 lamellas modified g-C_3N_4/$SrTiO_3$ core-shell heterojunction, Renewable Energy 161 (2020) 340-349.
[39] M. Inagaki, T. Tsumura, T. Kinumoto, M. Toyoda, Graphitic carbon nitrides (g-C_3N_4) with comparative discussion to carbon materials, Carbon 141 (2019) 580-607.
[40] H. Tang, S. Chang, G. Tang, W. Liang, AgBr and g-C_3N_4 co-modified Ag_2CO_3 photocatalyst: a novel multi-heterostructured photocatalyst with enhanced photocatalytic activity, Applied Surface Science 391 (2017) 440-448.
[41] G. Wang, X. Li, P. Hao, W. Liu, H. Zhan, S. Bi, g-C_3N_4/Nitrogen-Doped Carbon Dot/Silver Nanoparticle-Based Ternary Photocatalyst for Water Pollutant Treatment, ACS Applied Nano Materials 6(7) (2023) 5747-5758.
[42] Y. Zhang, J. Liu, G. Wu, W. Chen, Porous graphitic carbon nitride synthesized via direct polymerization of urea for efficient sunlight-driven photocatalytic hydrogen production, Nanoscale 4(17) (2012) 5300-5303.
[43] H. Dong, X. Guo, C. Yang, Z. Ouyang, Synthesis of g-C_3N_4 by different precursors under burning explosion effect and its photocatalytic degradation for tylosin, Applied Catalysis B: Environmental 230 (2018) 65-76.
[44] Z. Zhao, Y. Ma, J. Fan, Y. Xue, H. Chang, Y. Masubuchi, S. Yin, Synthesis of graphitic carbon nitride from different precursors by fractional thermal polymerization method and their visible light induced photocatalytic activities, Journal of Alloys and Compounds 735 (2018) 1297-1305.
[45] W.-J. Ong, L.-L. Tan, Y.H. Ng, S.-T. Yong, S.-P. Chai, Graphitic carbon nitride (g-C_3N_4)-based photocatalysts for artificial photosynthesis and environmental remediation: are we a step closer to achieving sustainability?, Chemical reviews 116(12) (2016) 7159-7329.
[46] Z. Mo, X. She, Y. Li, L. Liu, L. Huang, Z. Chen, Q. Zhang, H. Xu, H. Li, Synthesis of gC_3N_4 at different temperatures for superior visible/UV photocatalytic performance and photoelectrochemical sensing of MB solution, RSC advances 5(123) (2015) 101552-101562.
[47] Q. Tay, P. Kanhere, C.F. Ng, S. Chen, S. Chakraborty, A.C.H. Huan, T.C. Sum, R. Ahuja, Z. Chen, Defect engineered g-C_3N_4 for efficient visible light photocatalytic hydrogen production, Chemistry of Materials 27(14) (2015) 4930-4933.
[48] J. Xu, M. Fujitsuka, S. Kim, Z. Wang, T. Majima, Unprecedented effect of CO_2 calcination atmosphere on photocatalytic H_2 production activity from water using g-C_3N_4 synthesized from triazole polymerization, Applied Catalysis B: Environmental 241 (2019) 141-148.
[49] I. Khan, M. Luo, S. Khan, H. Asghar, M. Saeed, S. Khan, A. Khan, M. Humayun, L. Guo, B. Shi, Green synthesis of SrO bridged $LaFeO_3$/g-C_3N_4 nanocomposites for CO_2 conversion and bisphenol A degradation with new insights into mechanism, Environmental Research 207 (2022) 112650.
[50] S. Zhang, Y. Liu, P. Gu, R. Ma, T. Wen, G. Zhao, L. Li, Y. Ai, C. Hu, X. Wang, Enhanced photodegradation of toxic organic pollutants using dual-oxygen-doped porous g-C_3N_4: Mechanism exploration from both experimental and DFT studies, Applied Catalysis B: Environmental 248 (2019) 1-10.
[51] B. Zhou, M. Waqas, B. Yang, K. Xiao, S. Wang, C. Zhu, J. Li, J. Zhang, Convenient one-step fabrication and morphology evolution of thin-shelled honeycomb-like structured g-C_3N_4 to significantly enhance photocatalytic hydrogen evolution, Applied Surface Science 506 (2020) 145004.
[52] S. Zhang, S. Song, P. Gu, R. Ma, D. Wei, G. Zhao, T. Wen, R. Jehan, B. Hu, X. Wang, Visible-light-driven activation of persulfate over cyano and hydroxyl group co-modified mesoporous gC_3N_4 for boosting bisphenol A degradation, Journal of Materials Chemistry A 7(10) (2019) 5552-5560.
[53] C. Prasad, H. Tang, Q. Liu, I. Bahadur, S. Karlapudi, Y.J.i.j.o.h.e. Jiang, A latest overview on photocatalytic application of g-C_3N_4 based nanostructured materials for hydrogen production, 45(1) (2020) 337-379.
[54] X. Wang, X. Li, J. Wang, H. Zhu, Recent advances in carbon nitride-based nanomaterials for the removal of heavy metal ions from aqueous solution, Journal of Inorganic Materials 35(3) (2020) DOI: https://doi.org/10.15541/jim20190436.
[55] C. Bhuvaneswari, S.G. Babu, Nanoarchitecture and surface engineering strategy for the construction of 3D hierarchical CuS-rGO/g-C_3N_4 nanostructure: An ultrasensitive and highly selective electrochemical sensor for the detection of furazolidone drug, Journal of Electroanalytical Chemistry 907 (2022) 116080.
[56] C. Li, Z. Sun, Y. Xue, G. Yao, S. Zheng, A facile synthesis of g-C_3N_4/TiO_2 hybrid photocatalysts by sol–gel method and its enhanced photodegradation towards methylene blue under visible light, Advanced Powder Technology 27(2) (2016) 330-337.
[57] X. Liu, N. Chen, Y. Li, D. Deng, X. Xing, Y. Wang, A general nonaqueous sol-gel route to g-C_3N_4-coupling photocatalysts: the case of Z-scheme g-C_3N_4/TiO_2 with enhanced photodegradation toward RhB under visible-light, Scientific Reports 6(1) (2016) 39531.
[58] F. Chang, J. Zhang, Y. Xie, J. Chen, C. Li, J. Wang, J. Luo, B. Deng, X. Hu, Fabrication, characterization, and photocatalytic performance of exfoliated g-C_3N_4–TiO_2 hybrids, Applied Surface Science 311 (2014) 574-581.
[59] F. Deng, L. Zhao, X. Pei, X. Luo, S. Luo, Facile in situ hydrothermal synthesis of g-C_3N_4/SnS_2 composites with excellent visible-light photocatalytic activity, Materials Chemistry and Physics 189 (2017) 169-175.
[60] V. Harish, M. Ansari, D. Tewari, A.B. Yadav, N. Sharma, S. Bawarig, M.-L. García-Betancourt, A. Karatutlu, M. Bechelany, A. Barhoum, Cutting-edge advances in tailoring size, shape, and functionality of nanoparticles and nanostructures: A review, Journal of the Taiwan Institute of Chemical Engineers 149 (2023) 105010.
[61] N. Cheng, J. Tian, Q. Liu, C. Ge, A.H. Qusti, A.M. Asiri, A.O. Al-Youbi, X. Sun, interfaces, Au-nanoparticle-loaded graphitic carbon nitride nanosheets: green photocatalytic synthesis and application toward the degradation of organic pollutants, ACS Applied Materials & Interfaces 5(15) (2013) 6815-6819.
[62] J. Di, J. Xia, S. Yin, H. Xu, L. Xu, Y. Xu, M. He, H. Li, Preparation of sphere-like gC_3N_4/BiOI photocatalysts via a reactable ionic liquid for visible-light-driven photocatalytic degradation of pollutants, Journal of Materials chemistry A 2(15) (2014) 5340-5351.
[63] Y. Zhang, Y. Xu, L. Gao, X. Liu, Y. Fu, C. Ma, Y. Ge, R. Cao, X. Zhang, O.A. Al-Hartomy, S. Wageh, A. Al-Ghamdi, H. Algarni, Z. Shi, H. Zhang, MXene-based mixed-dimensional Schottky heterojunction towards self-powered flexible high-performance photodetector, Materials Today Physics 21 (2021) 100479.
[64] S. Meng, Y. Cui, H. Wang, X. Zheng, X. Fu, S. Chen, Noble metal-free 0D–1D NiS_x/CdS nanocomposites toward highly efficient photocatalytic contamination removal and hydrogen evolution under visible light, Dalton Transactions 47(36) (2018) 12671-12683.
[65] O.J. Ajala, J.O. Tijani, M.T. Bankole, A.S. Abdulkareem, A critical review on graphene oxide nanostructured material: Properties, Synthesis, characterization and application in water and wastewater treatment, Environmental Nanotechnology, Monitoring & Management 18 (2022) 100673.
[66] Z. Talebzadeh, M. Masjedi-Arani, O. Amiri, M. Salavati-Niasari, La2Sn2O7/g-C_3N_4 nanocomposites: Rapid and green sonochemical fabrication and photo-degradation performance for removal of dye contaminations, Ultrasonics Sonochemistry 77 (2021) 105678.
[67] M.A. Tekalgne, S.Y. Kim, Research progress and perspectives on photocatalysts based on the lead-free double halide perovskite, EES Catalysis (2024).
[68] M.S. Umekar, G.S. Bhusari, T. Bhoyar, V. Devthade, B.P. Kapgate, A.P. Potbhare, R.G. Chaudhary, A.A. Abdala, Graphitic carbon nitride-based photocatalysts for environmental remediation of organic pollutants, Current Nanoscience 19(2) (2023) 148-169.
[69] Y. Zhen, C. Yang, H. Shen, W. Xue, C. Gu, J. Feng, Y. Zhang, F. Fu, Y. Liang, Photocatalytic performance and mechanism insights of a S-scheme g-C_3N_4/Bi_2MoO_6 heterostructure in phenol degradation and hydrogen evolution reactions under visible light, Physical Chemistry Chemical Physics 22(45) (2020) 26278-26288.
[70] D. Zhu, Q. Zhou, Nitrogen doped g-C_3N_4 with the extremely narrow band

gap for excellent photocatalytic activities under visible light, Applied Catalysis B: Environmental 281 (2021) 119474.
[71] R. Acharya, K. Parida, A review on TiO_2/g-C_3N_4 visible-light-responsive photocatalysts for sustainable energy generation and environmental remediation, Journal of Environmental Chemical Engineering 8(4) (2020) 103896.
[72] H. Zhang, L. Jia, P. Wu, R. Xu, J. He, W. Jiang, Improved H_2O_2 photogeneration by KOH-doped g-C_3N_4 under visible light irradiation due to synergistic effect of N defects and K modification, Applied Surface Science 527 (2020) 146584.
[73] H. Liu, J. Liang, J. Du, Q. Gao, S. Fu, L. Li, M. Hu, F. Zhao, J. Zhou, Promoting charge separation in dual defect mediated Z-scheme MoS2/g-C3N4 photocatalysts for enhanced photocatalytic degradation activity: synergistic effect insight, Colloids and Surfaces A: Physicochemical and Engineering Aspects 594 (2020) 124668.
[74] D. Wang, J. Chen, X. Gao, Y. Ao, P. Wang, Maximizing the utilization of photo-generated electrons and holes of g-C_3N_4 photocatalyst for harmful algae inactivation, Chemical Engineering Journal 431 (2022) 134105.
[75] A. Mehtab, S.M. Alshehri, T. Ahmad, Photocatalytic and photoelectrocatalytic water splitting by porous g-C_3N_4 nanosheets for hydrogen generation, ACS Applied Nano Materials 5(9) (2022) 12656-12665.
[76] P. Murugesan, J. Moses, C. Anandharamakrishnan, Photocatalytic disinfection efficiency of 2D structure graphitic carbon nitride-based nanocomposites: a review, Journal of Materials Science 54(19) (2019) 12206-12235.
[77] C. Zhang, Y. Li, D. Shuai, Y. Shen, W. Xiong, L. Wang, Graphitic carbon nitride (g-C_3N_4)-based photocatalysts for water disinfection and microbial control: A review, Chemosphere 214 (2019) 462-479
[78] T. Lin, Z. Song, Y. Wu, L. Chen, S. Wang, F. Fu, L. Guo, Boron-and phenyl-codoped graphitic carbon nitride with greatly enhanced light responsive range for photocatalytic disinfection, Journal of Hazardous Materials 358 (2018) 62-68
[79] J.H. Thurston, N.M. Hunter, K.A. Cornell, Preparation and characterization of photoactive antimicrobial graphitic carbon nitride (g-C_3N_4) films, RSC advances 6(48) (2016) 42240-42248.
[80] Z. Liu, J. Wang, B. Kong, Z. Liu, T.-t. Song, W. Wang, Evidence of direct Z-scheme triazine-based gC_3N_4/BiOI (001) heterostructures: a hybrid density functional investigation, Physical Chemistry Chemical Physics 25(1) (2023) 847-856.
[81] J. Zou, G. Liao, J. Jiang, Z. Xiong, S. Bai, H. Wang, P. Wu, P. Zhang, X. Li, In-situ construction of sulfur-doped g-C_3N_4/defective g-C_3N_4 isotype step-scheme heterojunction for boosting photocatalytic H2 evolution, Chinese Journal of Structural Chemistry 41(1) (2022) 2201025-2201033.
[82] P. Mandyal, A. Guleria, R. Sharma, S. Sambyal, A. Priye, B. Fang, P. Shandilya, Insight into the properties, morphologies and photocatalytic applications of S-scheme Bi2WO6, Journal of Environmental Chemical Engineering (2022) 108918.
[83] M. Muhyuddin, G. Tseberlidis, M. Acciarri, O. Lori, M. D'Arienzo, M. Cavallini, P. Atanassov, L. Elbaz, A. Lavacchi, C. Santoro, Molybdenum disulfide as hydrogen evolution catalyst: From atomistic to materials structure and electrocatalytic performance, Journal of Energy Chemistry (2023).
[84] M. Ismael, Environmental remediation and sustainable energy generation via photocatalytic technology using rare earth metals modified g-C_3N_4: A review, Journal of Alloys and Compounds 931 (2023) 167469.
[85] M. Jyothi, V. Nayak, K.R. Reddy, S. Naveen, A. Raghu, Non-metal (oxygen, sulphur, nitrogen, boron and phosphorus)-doped metal oxide hybrid nanostructures as highly efficient photocatalysts for water treatment and hydrogen generation, Nanophotocatalysis and Environmental Applications: Materials and Technology (2019) 83-105.
[86] C. Prasad, H. Tang, Q. Liu, I. Bahadur, S. Karlapudi, Y. Jiang, A latest overview on photocatalytic application of g-C_3N_4 based nanostructured materials for hydrogen production, international journal of hydrogen energy 45(1) (2020) 337-379.
[87] X. Liu, L. Rao, Y. Yao, H. Chen, Phosphorus-doped carbon fibers as an efficient metal-free bifunctional catalyst for removing sulfamethoxazole and chromium (VI), Chemosphere 246 (2020) 125783.
[88] T. Zahra, K.S. Ahmad, C. Zequine, R.K. Gupta, A.G. Thomas, M.A. Malik, S.B. Jaffri, D. Ali, Electro-catalyst [ZrO_2/ZnO/PdO]-NPs green functionalization: fabrication, characterization and water splitting potential assessment, International Journal of Hydrogen Energy 46(37) (2021) 19347-19362.
[89] N.A.R. Che Mohamad, F. Marques Mota, D.H. Kim, Photocatalytic and Photoelectrochemical Overall Water Splitting, Solar-to-Chemical Conversion: Photocatalytic and Photoelectrochemcial Processes (2021) 189-242.
[90] G. Dong, K. Zhao, L. Zhang, Carbon self-doping induced high electronic conductivity and photoreactivity of gC_3N_4, Chemical communications 48(49) (2012) 6178-6180.
[91] F. Dong, Y. Li, Z. Wang, W.-K. Ho, Enhanced visible light photocatalytic activity and oxidation ability of porous graphene-like g-C_3N_4 nanosheets via thermal exfoliation, Applied Surface Science 358 (2015) 393-403.
[92] F. Zuo, L. Wang, T. Wu, Z. Zhang, D. Borchardt, P. Feng, Self-doped Ti3+ enhanced photocatalyst for hydrogen production under visible light, Journal of the American Chemical Society 132(34) (2010) 11856-11857.
[93] A. Kumar, P. Raizada, P. Singh, R.V. Saini, A.K. Saini, A. Hosseini-Bandegharaei, Perspective and status of polymeric graphitic carbon nitride based Z-scheme photocatalytic systems for sustainable photocatalytic water purification, Chemical Engineering Journal 391 (2020) 123496.
[94] Y. Pang, Y. Li, G. Xu, Y. Hu, Z. Kou, Q. Feng, J. Lv, Y. Zhang, J. Wang, Y. Wu, Z-scheme carbon-bridged Bi_2O_3/TiO_2 nanotube arrays to boost photoelectrochemical detection performance, Applied Catalysis B: Environmental 248 (2019) 255-263.
[95] J. Wu, Y. Zhang, T. Wang, Y. Xin, D. Ma, Au nanoparticles and graphene oxide co-loaded graphitic carbon nitride: Synthesis and photocatalytic application, Materials Research Bulletin 100 (2018) 282-288.
[96] C. Daulbayev, F. Sultanov, B. Bakbolat, O. Daulbayev, 0D, 1D and 2D nanomaterials for visible photoelectrochemical water splitting. A review, International Journal of Hydrogen Energy 45(58) (2020) 33325-33342.
[97] H. Zhang, Y. Tang, Z. Liu, Z. Zhu, X. Tang, Y. Wang, Study on optical properties of alkali metal doped g-C_3N_4 and their photocatalytic activity for reduction of CO_2, Chemical Physics Letters 751 (2020) 137467.
[98] S. Zhang, P. Gu, R. Ma, C. Luo, T. Wen, G. Zhao, W. Cheng, X. Wang, Recent developments in fabrication and structure regulation of visible-light-driven g-C3N4-based photocatalysts towards water purification: a critical review, Catalysis Today 335 (2019) 65-77.
[99] Q. Zhu, Y. Xuan, K. Zhang, K. Chang, Enhancing photocatalytic CO_2 reduction performance of g-C_3N_4-based catalysts with non-noble plasmonic nanoparticles, Applied Catalysis B: Environmental 297 (2021) 120440.
[100] Y. Fu, T. Huang, L. Zhang, J. Zhu, X. Wang, Ag/gC_3N_4 catalyst with superior catalytic performance for the degradation of dyes: a borohydride-generated superoxide radical approach, Nanoscale 7(32) (2015) 13723-13733.
[101] S. Tonda, S. Kumar, V. Shanker, Surface plasmon resonance-induced photocatalysis by Au nanoparticles decorated mesoporous g-C_3N_4 nanosheets under direct sunlight irradiation, Materials Research Bulletin 75 (2016) 51-58.
[102] S. Zhang, B. Li, X. Wang, G. Zhao, B. Hu, Z. Lu, T. Wen, J. Chen, X. Wang, Recent developments of two-dimensional graphene-based composites in visible-light photocatalysis for eliminating persistent organic pollutants from wastewater, Chemical Engineering Journal 390 (2020) 124642.
[103] M.B. Gawande, A. Goswami, F.-X. Felpin, T. Asefa, X. Huang, R. Silva, X. Zou, R. Zboril, R.S. Varma, Cu and Cu-based nanoparticles: synthesis and applications in catalysis, Chemical Reviews 116(6) (2016) 3722-3811.
[104] Y. Liu, Y. Zheng, W. Zhang, Z. Peng, H. Xie, Y. Wang, X. Guo, M. Zhang, R. Li, Y. Huang, Template-free preparation of non-metal (B, P, S) doped g-C_3N_4 tubes with enhanced photocatalytic H_2O_2 generation, Journal of Materials Science & Technology 95 (2021) 127-135.
[105] M.S. Nasir, G. Yang, I. Ayub, S. Wang, W. Yan, In situ decoration of g-C_3N_4 quantum dots on 1D branched TiO_2 loaded with plasmonic Au nanoparticles and improved the photocatalytic hydrogen evolution activity, Applied Surface Science 519 (2020) 146208.
[106] G. Xu, Y. Xu, Z. Zhou, Y. Bai, Facile hydrothermal preparation of graphitic carbon nitride supercell structures with enhanced photodegradation activity, Diamond and Related Materials 97 (2019) 107461.
[107] Q. Xie, W. He, S. Liu, C. Li, J. Zhang, P.K. Wong, Bifunctional S-scheme g-C_3N_4/Bi/BiVO4 hybrid photocatalysts toward artificial carbon cycling, Chinese Journal of Catalysis 41(1) (2020) 140-153.
[108] X. He, S. Bai, J. Jiang, W.-J. Ong, J. Peng, Z. Xiong, G. Liao, J. Zou, N. Li, Oxygen vacancy mediated step-scheme heterojunction of WO_2. 9/g-C_3N_4 for efficient electrochemical sensing of 4-nitrophenol, Chemical Engineering Journal Advances 8 (2021) 100175.
[109] X. Zhu, Y. Wang, Y. Guo, J. Wan, Y. Yan, Y. Zhou, C. Sun, Environmental-friendly synthesis of heterojunction photocatalysts g-C_3N_4/$BiPO_4$ with enhanced photocatalytic performance, Applied Surface Science 544 (2021) 148872.
[110] S. Patnaik, S. Martha, S. Acharya, K. Parida, An overview of the modification of g-C_3N_4 with high carbon containing materials for photocatalytic applications, Separation and Purification Technology 3(3) (2016) 336-347.
[111] J. Wen, J. Xie, X. Chen, X. Li, A review on g-C_3N_4-based photocatalysts, Applied Surface Science 391 (2017) 72-123.
[112] S. Kumar, S. Karthikeyan, A.F. Lee, g-C_3N_4-based nanomaterials for visible light-driven photocatalysis, Catalysts 8(2) (2018) 74.
[113] F. Pei, S. Feng, Y. Wu, X. Lv, H. Wang, S.-M. Chen, Q. Hao, Y. Cao, W. Lei, Z. Tong, Label-free photoelectrochemical immunosensor for aflatoxin B1 detec-

tion based on the Z-scheme heterojunction of g-C_3N_4/Au/WO_3, Biosensors and Bioelectronics 189 (2021) 113373.
[114] L. Wang, Y. Li, P. Han, Electrospinning preparation of g-C_3N_4/Nb_2O_5 nanofibers heterojunction for enhanced photocatalytic degradation of organic pollutants in water, Scientific Reports 11(1) (2021) 22950.
[115] J. Ren, S. Lv, S. Wang, M. Bao, X. Zhang, Y. Gao, Y. Liu, Z. Zhang, L. Zeng, J. Ke, Construction of efficient g-C_3N_4/NH_2-UiO-66 (Zr) heterojunction photocatalysts for wastewater purification, Separation and Purification Technology 274 (2021) 118973.
[116] J. Liao, W. Cui, J. Li, J. Sheng, H. Wang, P. Chen, G. Jiang, Z. Wang, F. Dong, Nitrogen defect structure and NO+ intermediate promoted photocatalytic NO removal on H2 treated g-C_3N_4, Chemical Engineering Journal 379 (2020) 122282.
[117] W.-D. Oh, L.-W. Lok, A. Veksha, A. Giannis, T.-T. Lim, Enhanced photocatalytic degradation of bisphenol A with Ag-decorated S-doped g-C_3N_4 under solar irradiation: performance and mechanistic studies, Chemical Engineering Journal 333 (2018) 739-749.
[118] L. Liu, J. Huang, H. Yu, J. Wan, L. Liu, K. Yi, W. Zhang, C. Zhang, Construction of MoO3 nanoparticles/g-C_3N_4 nanosheets 0D/2D heterojuntion photocatalysts for enhanced photocatalytic degradation of antibiotic pollutant, Chemosphere 282 (2021) 131049.
[119] P. Niu, L.C. Yin, Y.Q. Yang, G. Liu, H.M. Cheng, Increasing the visible light absorption of graphitic carbon nitride (Melon) photocatalysts by homogeneous self-modification with nitrogen vacancies, Advanced Materials 26(47) (2014) 8046-8052.
[120] J. Wu, N. Li, H.-B. Fang, X. Li, Y.-Z. Zheng, X. Tao, Nitrogen vacancies modified graphitic carbon nitride: Scalable and one-step fabrication with efficient visible-light-driven hydrogen evolution, Chemical Engineering Journal 358 (2019) 20-29.
[121] J. Ding, W. Xu, H. Wan, D. Yuan, C. Chen, L. Wang, G. Guan, W.-L. Dai, Nitrogen vacancy engineered graphitic C_3N_4-based polymers for photocatalytic oxidation of aromatic alcohols to aldehydes, Applied Catalysis B: Environmental 221 (2018) 626-634.
[122] Z. Wang, Y. Huang, M. Chen, X. Shi, Y. Zhang, J. Cao, W. Ho, S.C. Lee, Roles of N-vacancies over porous g-C_3N_4 microtubes during photocatalytic NOx removal, ACS Applied Materials & Interfaces 11(11) (2019) 10651-10662.
[123] D. Chen, J. Yang, H. Ding, Synthesis of nanoporous carbon nitride using calcium carbonate as templates with enhanced visible-light photocatalytic activity, Applied Surface Science 391 (2017) 384-391.
[124] Y. Yang, L. Geng, Y. Guo, J. Meng, Y. Guo, Easy dispersion and excellent visible-light photocatalytic activity of the ultrathin urea-derived g-C_3N_4 nanosheets, Applied Surface Science 425 (2017) 535-546.
[125] X. Wang, Q. Liu, Q. Yang, Z. Zhang, X. Fang, Three-dimensional g-C_3N_4 aggregates of hollow bubbles with high photocatalytic degradation of tetracycline, Carbon 136 (2018) 103-112.
[126] Z. Jin, Q. Zhang, S. Yuan, T. Ohno, Synthesis high specific surface area nanotube gC_3N_4 with two-step condensation treatment of melamine to enhance photocatalysis properties, Rsc Advances 5(6) (2015) 4026-4029.
[127] C. Fan, Q. Feng, G. Xu, J. Lv, Y. Zhang, J. Liu, Y. Qin, Y. Wu, Enhanced photocatalytic performances of ultrafine g-C_3N_4 nanosheets obtained by gaseous stripping with wet nitrogen, Applied Surface Science 427 (2018) 730-738.
[128] T. Yu, T. Xie, W. Zhou, Y. Zhang, Y. Chen, B. Shao, W.-Q. Guo, X. Tan, Fumaric acid assistant band structure tunable nitrogen defective g-C_3N_4 fabrication for enhanced photocatalytic hydrogen evolution, ACS Sustainable Chemistry & Engineering 9(22) (2021) 7529-7540.
[129] Y. Qin, J. Lu, X. Zhao, X. Lin, Y. Hao, P. Huo, M. Meng, Y. Yan, Nitrogen defect engineering and π-conjugation structure decorated g-C_3N_4 with highly enhanced visible-light photocatalytic hydrogen evolution and mechanism insight, Chemical Engineering Journal 425 (2021) 131844.
[130] A. Torres-Pinto, A.M. Díez, C.G. Silva, J.L. Faria, M.Á. Sanromán, A.M. Silva, M. Pazos, Photoelectrocatalytic degradation of pharmaceuticals promoted by a metal-free gC_3N_4 catalyst, Chemical Engineering Journal 476 (2023) 146761.
[131] A. Balakrishnan, M. Chinthala, R.K. Polagani, D.-V.N. Vo, Removal of tetracycline from wastewater using g-C_3N_4 based photocatalysts: A review, Environmental Research 216 (2023) 114660.
[132] D. Ramírez-Morales, M. Masís-Mora, J.R. Montiel-Mora, M. Méndez-Rivera, J.A. Gutiérrez-Quirós, L. Brenes-Alfaro, C.E. Rodríguez-Rodríguez, Pharmaceuticals, hazard and ecotoxicity in surface and wastewater in a tropical dairy production area in Latin America, Chemosphere (2023) 140443.
[133] G.Z.S. Ling, S.F. Ng, W.J. Ong, Tailor-engineered 2D cocatalysts: harnessing electron–hole redox center of 2D g-C_3N_4 photocatalysts toward solar-to-chemical conversion and environmental purification, Advanced Functional Materials 32(29) (2022) 2111875.
[134] P. Gan, Y. Lu, Y. Li, W. Liu, L. Chen, M. Tong, J. Liang, Non-radical degradation of organic pharmaceuticals by g-C_3N_4 under visible light irradiation: The overlooked role of excitonic energy transfer, Journal of Hazardous Materials 445 (2023) 130549.
[135] J. Rashid, A. Abbas, L.C. Chang, A. Iqbal, I.U. Haq, A. Rehman, S.U. Awan, M. Arshad, M. Rafique, M. Barakat, Butterfly cluster like lamellar BiOBr/TiO_2 nanocomposite for enhanced sunlight photocatalytic mineralization of aqueous ciprofloxacin, Science of the Total Environment 665 (2019) 668-677.
[136] Y. Zhou, L. Zhou, C. Ni, E. He, L. Yu, X. Li, 3D/2D MOF-derived Co-CeOx/g-C_3N_4 Z-scheme heterojunction for visible light photocatalysis: Hydrogen production and degradation of carbamazepine, Journal of Alloys and Compounds 890 (2022) 161786.
[137] E. Cako, S. Dudziak, P. Głuchowski, G. Trykowski, M. Pisarek, A.F. Borzyszkowska, K. Sikora, A. Zielińska-Jurek, Heterojunction of (P, S) co-doped g-C_3N_4 and 2D TiO_2 for improved carbamazepine and acetaminophen photocatalytic degradation, Separation and Purification Technology 311 (2023) 123320.
[138] E.S. Okeke, K.I. Chukwudozie, R. Nyaruaba, R.E. Ita, A. Oladipo, O. Ejeromedoghene, E.O. Atakpa, C.V. Agu, C.O. Okoye, Antibiotic resistance in aquaculture and aquatic organisms: a review of current nanotechnology applications for sustainable management, Environmental Science and Pollution Research 29(46) (2022) 69241-69274.
[139] X. Yang, Z. Chen, W. Zhao, C. Liu, X. Qian, M. Zhang, G. Wei, E. Khan, Y.H. Ng, Y.S. Ok, Recent advances in photodegradation of antibiotic residues in water, Chemical Engineering Journal 405 (2021) 126806.
[140] S.K. Fanourakis, J. Peña-Bahamonde, P.C. Bandara, D.F. Rodrigues, Nano-based adsorbent and photocatalyst use for pharmaceutical contaminant removal during indirect potable water reuse, NPJ Clean Water 3(1) (2020) 1.
[141] Y. Liu, X. Zeng, X. Hu, J. Hu, Z. Wang, Y. Yin, C. Sun, X. Zhang, Two-dimensional g-C_3N4/TiO_2 nanocomposites as vertical Z-scheme heterojunction for improved photocatalytic water disinfection, Catalysis Today 335 (2019) 243-251.
[142] H. Zhang, W. Wu, Y. Li, Y. Wang, C. Zhang, W. Zhang, L. Wang, L. Niu, Enhanced photocatalytic degradation of ciprofloxacin using novel C-dot@ Nitrogen deficient g-C_3N_4: synergistic effect of nitrogen defects and C-dots, Applied Surface Science 465 (2019) 450-458.
[143] H. Li, Y. Gao, X. Wu, P.-H. Lee, K. Shih, Fabrication of heterostructured g-C_3N_4/Ag-TiO_2 hybrid photocatalyst with enhanced performance in photocatalytic conversion of CO_2 under simulated sunlight irradiation, Applied Surface Science 402 (2017) 198-207.
[144] H. Liang, J. Guo, M. Yu, Y. Zhou, R. Zhan, C. Liu, J. Niu, Porous loofah-sponge-like ternary heterojunction g-C_3N_4/Bi_2WO_6/MoS_2 for highly efficient photocatalytic degradation of sulfamethoxazole under visible-light irradiation, Chemosphere 279 (2021) 130552.
[145] N. Lu, P. Wang, Y. Su, H. Yu, N. Liu, X. Quan, Construction of Z-Scheme g-C_3N_4/RGO/WO_3 with in situ photoreduced graphene oxide as electron mediator for efficient photocatalytic degradation of ciprofloxacin, Chemosphere 215 (2019) 444-453.
[146] J. Huang, W. Chen, X. Yu, X. Fu, Y. Zhu, Y. Zhang, Fabrication of a ternary BiOCl/CQDs/rGO photocatalyst: The roles of CQDs and rGO in adsorption-photocatalytic removal of ciprofloxacin, Colloids and Surfaces A: Physicochemical and Engineering Aspects 597 (2020) 124758.
[147] N. Roy, S.A. Alex, N. Chandrasekaran, A. Mukherjee, K. Kannabiran, A comprehensive update on antibiotics as an emerging water pollutant and their removal using nano-structured photocatalysts, Journal of Environmental Chemical Engineering 9(2) (2021) 104796.
[148] M. Verma, A. Haritash, Photocatalytic degradation of Amoxicillin in pharmaceutical wastewater: A potential tool to manage residual antibiotics, Environmental Technology & Innovation 20 (2020) 101072.
[149] S. Shenoy, C. Chuaicham, T. Okumura, K. Sekar, K. Sasaki, Simple tactic polycondensation synthesis of Z-scheme quasi-polymeric g-C_3N_4/$CaFe_2O_4$ composite for enhanced photocatalytic water depollution via pn heterojunction, Chemical Engineering Journal 453 (2023) 139758.
[150] Z. Hu, X. Cai, Z. Wang, S. Li, Z. Wang, X. Xie, Construction of carbon-doped supramolecule-based g-C_3N_4/TiO_2 composites for removal of diclofenac and carbamazepine: A comparative study of operating parameters, mechanisms, degradation pathways, Journal of hazardous materials 380 (2019) 120812.
[151] X. Wang, P. Zhang, L. Li, N. Li, X. Su, X. Wei, L. Han, Preparation of a high-performance N-defect ZnO@ g-C_3N_4 nanocomposite and its photocatalytic degradation of tetracycline, Materials Today Communications 36 (2023) 106732.
[152] M. Yu, H. Liang, R. Zhan, L. Xu, J. Niu, Sm-doped g-C_3N_4/Ti_3C_2 MXene heterojunction for visible-light photocatalytic degradation of ciprofloxacin, Chinese Chemical Letters 32(7) (2021) 2155-2158.

[153] I. Ihsanullah, MXenes as next-generation materials for the photocatalytic degradation of pharmaceuticals in water, Journal of Environmental Chemical Engineering 10(3) (2022) 107381.
[154] S. Lu, C. Li, H. Li, Y. Zhao, Y. Gong, L. Niu, X. Liu, T. Wang, The effects of nonmetal dopants on the electronic, optical and chemical performances of monolayer g–C_3N_4 by first-principles study, Applied Surface Science 392 (2017) 966-974.
[155] K. Hu, R. Li, C. Ye, A. Wang, W. Wei, D. Hu, R. Qiu, K. Yan, Facile synthesis of Z-scheme composite of TiO_2 nanorod/g-C_3N_4 nanosheet efficient for photocatalytic degradation of ciprofloxacin, Journal of Cleaner Production 253 (2020) 120055.
[156] L.K.B. Paragas, V. Dien Dang, R.S. Sahu, S. Garcia-Segura, M.D.G. de Luna, J.A.I. Pimentel, R.-A. Doong, Enhanced visible-light-driven photocatalytic degradation of acetaminophen over CeO_2/I, K-codoped C_3N_4 heterojunction with tunable properties in simulated water matrix, Separation and Purification Technology 272 (2021) 117567.
[157] H.N. Phong Vo, G.K. Le, T.M. Hong Nguyen, X.-T. Bui, K.H. Nguyen, E.R. Rene, T.D.H. Vo, N.-D. Thanh Cao, R. Mohan, Acetaminophen micropollutant: Historical and current occurrences, toxicity, removal strategies and transformation pathways in different environments, Chemosphere 236 (2019) 124391.
[158] E. Brillas, J. Manuel Peralta-Hernández, Removal of paracetamol (acetaminophen) by photocatalysis and photoelectrocatalysis. A critical review, Separation and Purification Technology 309 (2023) 122982.
[159] M. Noorisepehr, B. Kakavandi, A.A. Isari, F. Ghanbari, E. Dehghanifard, N. Ghomi, F. Kamrani, Sulfate radical-based oxidative degradation of acetaminophen over an efficient hybrid system: Peroxydisulfate decomposed by ferroferric oxide nanocatalyst anchored on activated carbon and UV light, Separation and Purification Technology 250 (2020) 116950.
[160] K. Li, J. Chen, Y. Ao, P. Wang, Preparation of a ternary g-C_3N_4-CdS/Bi_4O5I_2 composite photocatalysts with two charge transfer pathways for efficient degradation of acetaminophen under visible light irradiation, Separation and Purification Technology 259 (2021) 118177.
[161] S. Moradi, A.A. Isari, F. Hayati, R. Rezaei Kalantary, B. Kakavandi, Co-implanting of TiO_2 and liquid-phase-delaminated g-C_3N_4 on multi-functional graphene nanobridges for enhancing photocatalytic degradation of acetaminophen, Chemical Engineering Journal 414 (2021) 128618.
[162] S. Gupta, J. Gandhi, S. Kokate, L.G. Raikar, V.G. Kopuri, H. Prakash, Augmented photocatalytic degradation of Acetaminophen using hydrothermally treated g-C_3N_4 and persulfate under LED irradiation, Heliyon 9(5) (2023).
[163] F.J. Benitez, J.L. Acero, F.J. Real, G. Roldan, E. Rodriguez, Photolysis of model emerging contaminants in ultra-pure water: Kinetics, by-products formation and degradation pathways, Water Research 47(2) (2013) 870-880.
[164] K. Perović, F.M. dela Rosa, M. Kovačić, H. Kušić, U.L. Štangar, F. Fresno, D.D. Dionysiou, A. Loncaric Bozic, Recent Achievements in Development of TiO_2-Based Composite Photocatalytic Materials for Solar Driven Water Purification and Water Splitting, Materials 13(6) (2020) 1338.
[165] A. Hayat, J.A. Shah Syed, A.G. Al-Sehemi, K.S. El-Nasser, T.A. Taha, A.A. Al-Ghamdi, M.A. Amin, Z. Ajmal, W. Iqbal, A. Palamanit, D.I. Medina, W.I. Nawawi, M. Sohail, State of the art advancement in rational design of g-C_3N_4 photocatalyst for efficient solar fuel transformation, environmental decontamination and future perspectives, International Journal of Hydrogen Energy 47(20) (2022) 10837-10867.
[166] M. Israel, P. Beaudry, Carbamazepine in Psychiatry: A Review, The Canadian Journal of Psychiatry 33(7) (1988) 577-584.
[167] K. Chojnacka, D. Skrzypczak, G. Izydorczyk, K. Mikula, D. Szopa, K. Moustakas, A. Witek-Krowiak, Biodegradation of pharmaceuticals in photobioreactors – a systematic literature review, Bioengineered 13(2) (2022) 4537-4556.
[168] M.N. Chong, B. Jin, G. Laera, C.P. Saint, Evaluating the photodegradation of Carbamazepine in a sequential batch photoreactor system: Impacts of effluent organic matter and inorganic ions, Chemical Engineering Journal 174(2) (2011) 595-602.
[169] Y. Zhang, S.-U. Geißen, C. Gal, Carbamazepine and diclofenac: Removal in wastewater treatment plants and occurrence in water bodies, Chemosphere 73(8) (2008) 1151-1161.
[170] A.S. Mestre, A.P. Carvalho, Photocatalytic Degradation of Pharmaceuticals Carbamazepine, Diclofenac, and Sulfamethoxazole by Semiconductor and Carbon Materials: A Review, Molecules 24(20) (2019) 3702.
[171] J. Deng, Y. Shao, N. Gao, S. Xia, C. Tan, S. Zhou, X. Hu, Degradation of the antiepileptic drug carbamazepine upon different UV-based advanced oxidation processes in water, Chemical Engineering Journal 222 (2013) 150-158.
[172] R. Kumar, M. Qureshi, D.K. Vishwakarma, N. Al-Ansari, A. Kuriqi, A. Elbeltagi, A. Saraswat, A review on emerging water contaminants and the application of sustainable removal technologies, Case Studies in Chemical and Environmental Engineering 6 (2022) 100219.
[173] P. Gan, Z. Zhang, Y. Hu, Y. Li, J. Ye, M. Tong, J. Liang, Insight into the role of Fe in the synergetic effect of persulfate/sulfite and Fe_2O_3@g-C_3N_4 for carbamazepine degradation, Science of The Total Environment 819 (2022) 152787.
[174] T. Xu, D. Wang, L. Dong, H. Shen, W. Lu, W. Chen, Graphitic carbon nitride co-modified by zinc phthalocyanine and graphene quantum dots for the efficient photocatalytic degradation of refractory contaminants, Applied Catalysis B: Environmental 244 (2019) 96-106.
[175] L. Yang, L. Liang, L. Wang, J. Zhu, S. Gao, X. Xia, Accelerated photocatalytic oxidation of carbamazepine by a novel 3D hierarchical protonated g-C_3N_4/BiOBr heterojunction: Performance and mechanism, Applied Surface Science 473 (2019) 527-539.
[176] X. Mei, S. Chen, G. Wang, W. Chen, W. Lu, B. Zhang, Y. Fang, C. Qi, Metal-free carboxyl modified g-C_3N_4 for enhancing photocatalytic degradation activity of organic pollutants through peroxymonosulfate activation in wastewater under solar radiation, Journal of Solid State Chemistry 310 (2022) 123053.
[177] Z. Cheng, L. Ling, J. Fang, C. Shang, Visible light-driven g-C_3N_4 peroxymonosulfate activation process for carbamazepine degradation: Activation mechanism and matrix effects, Chemosphere 286 (2022) 131906.
[178] T. Xia, Q. Hou, H. Qian, R. Lai, X. Bai, G. Yu, W. Zhang, M.L.U. Rehman, M. Ju, Fabricating metal-free Z-scheme heterostructures with nitrogen-deficient carbon nitride for fast photocatalytic removal of acetaminophen, Separation and Purification Technology 308 (2023) 122964.
[179] X. Du, X. Bai, L. Xu, L. Yang, P. Jin, Visible-light activation of persulfate by TiO_2/g-C_3N_4 photocatalyst toward efficient degradation of micropollutants, Chemical Engineering Journal 384 (2020) 123245.
[180] F. Al Marzouqi, R. Selvaraj, Y. Kim, Rapid photocatalytic degradation of acetaminophen and levofloxacin using g-C_3N_4 nanosheets under solar light irradiation, Materials Research Express 6(12) (2020) 125538.
[181] A. Hassani, P. Eghbali, B. Kakavandi, K.-Y.A. Lin, F. Ghanbari, Acetaminophen removal from aqueous solutions through peroxymonosulfate activation by CoFe2O4/mp g-C_3N_4 nanocomposite: Insight into the performance and degradation kinetics, Environmental Technology & Innovation 20 (2020) 101127.
[182] W. Hou, C. Deng, H. Xu, D. Li, Z. Zou, H. Xia, D. Xia, n–p BiOCl@ g-C_3N_4 Heterostructure with Rich-oxygen Vacancies for Photodegradation of Carbamazepine, ChemistrySelect 5(9) (2020) 2767-2777.
[183] F. Goudarzy, J. Zolgharnein, J.B. Ghasemi, Determination and degradation of carbamazepine using g-C_3N_4@ CuS nanocomposite as sensitive fluorescence sensor and efficient photocatalyst, Inorganic Chemistry Communications 141 (2022) 109512.
[184] N.S. Alhokbany, R. Mousa, M. Naushad, S.M. Alshehri, T. Ahamad, Fabrication of Z-scheme photocatalysts g-C_3N_4/Ag_3PO_4/chitosan for the photocatalytic degradation of ciprofloxacin, International Journal of Biological Macromolecules 164 (2020) 3864-3872.
[185] W. Shi, Y. Liu, W. Sun, Y. Hong, X. Li, X. Lin, F. Guo, J. Shi, Assembling g-C_3N_4 nanosheets on rod-like $CoFe_2O_4$ nanocrystals to boost photocatalytic degradation of ciprofloxacin with peroxymonosulfate activation, Materials Today Communications 29 (2021) 102871.
[186] H. Liang, M. Yu, J. Guo, R. Zhan, J. Chen, D. Li, L. Zhang, J. Niu, A novel vacancy-strengthened Z-scheme g-C_3N_4/Bp/MoS_2 composite for super-efficient visible-light photocatalytic degradation of ciprofloxacin, Separation and Purification Technology 272 (2021) 118891.
[187] J. Zhou, B. Zhu, Novel 1D/3D CeO_2/g-C_3N_4 catalysts for photodegradation of ciprofloxacin under visible light via dimensional regulation and heterostructure construction, Journal of Physics and Chemistry of Solids 171 (2022) 111002.